Treatment Performance of Direct Contact Membrane Distillation for Volatile, Semi-Volatile and Non-Volatile Organic Contaminants in Water

Danbi Won

A thesis

submitted for the partial fulfillment of the

requirements for the degree of

Master of Science
in Civil Engineering

University of Washington

2017

Committee:

Edward P. Kolodziej

Gregory V. Korshin

Program Authorized to Offer Degree:

Civil & Environmental Engineering

Abstract

Treatment Performance of Direct Contact Membrane Distillation for Broad Spectrum of Organic

Contaminants in Water

Danbi Won

Chair of Supervisory Committee: Edward P. Kolodziej
Department of Civil and Environmental Engineering

A laboratory-scale direct contact membrane distillation (DCMD) system was analyzed for treatment performances of a selection of volatile (V), semi-volatile (SV) and non-volatile (NV) organic contaminants, pharmaceuticals and personal care products (PPCPs) and nitrosamines that are of interest to water or wastewater treatment. A group of 32 organics, 8 nitrosamines, and 22 PPCPs were observed with acceptable mass recoveries ($> 60\%$) in the system, with observed recoveries well explained by their lower hydrophobicity (log Kow < 3) and less propensity to sorb to DCMD system components. Due to their low volatility, and consistent with expectations derived from Henry's law partitioning coefficients (K_H; where $pK_H = -\log K_H$), NV solutes with $pK_H > 8$ were rejected efficiently, with observed rejections of over 90%. Henry's Law constants estimated at 25°C were not fully predictive of treatment performance during DCMD, indicating that other physical and chemical characteristics contribute to rejection. For example, moderate rejections (i.e. 35% to 69%) were observed for some NV solutes with $pK_H < 8$, as the 50°C feed temperatures increased their apparent volatility in the system. Rejections for SV and V solutes were typically

lower, often more variable and sensitive to solute characteristics such as ionizability. In some cases, dissociation constants (pK_a) explained higher than expected rejection (e.g. 2-methyl-4,6-dinitrophenol; $pK_a = 4.31$) for ionizable solutes that were non-volatile at system pH. To account for the time dependent characteristics of DCMD batch system, a least square curve fitting modeling approach was used to evaluate the possibility for non-equilibrium, mass transfer limited conditions for SV and V solutes. Permeate fluxes of each contaminant also were developed based on observed DCMD data.

Acknowledgements

I am grateful to my adviser, Dr. Edward Kolodziej, for enabling and advising my research at the University of Washington. I would like to express my gratitude to my second committee member, Dr. Gregory Korshin, for his support through my master degree at the University of Washington.

I would like to thank research fellows, Dr. Sage R. Hiibel and Kevin A. Salls for their advice and contributions to my research.

I also wish to thank my family and fiancé for their incredible support and encouragement with their kind words throughout the duration of my studies. I would especially like to thank Bosun Gwon, Yongsuk Won, Hana Won, and Yoonbae Park.

Lastly, I wish to thank the United States Environmental Protection Agency Star Program for the research grant support, which spiced up my persistent research efforts and enables my success.

Table of Contents

List of Figures

List of Tables

Chapter 1. Introduction

Membrane distillation (MD) is capable of targeted separation of organic chemicals, metals, and salts to improve water quality of seawater or contaminated fresh waters. MD membranes are hydrophobic, with micron-scale non-wetted pores that enable vapor phase transport through the membrane after evaporation from the liquid phase. Unlike most membrane processes, MD membranes operate at atmospheric pressure, reducing pumping costs and limiting pressure driven accumulation of foulants at the membrane surface. Membrane distillation configurations include direct contact MD (DCMD), air gap MD (AGMD), vacuum MD (VMD), and sweeping gas MD (SWGMD).[1-2]

DCMD is the simplest configuration where the hydrophobic membrane is directly contacted with the warm feed and cool distillate solutions. Temperature differences between the feed and distillate surfaces in DCMD generate a partial vapor pressure difference across the membrane, which is the driving force for mass transfer of water and volatile solutes. DCMD is potentially a high efficiency separation process because increasing solute concentrations do not substantially alter the partial vapor pressure of water.[3] DCMD can be cost-effective because of its simplicity to set up and operate, and it is potentially suitable for waste heat capture because only a low temperature differential (20-50°C[1]) is required between feed and distillate. A solute, if volatile, transports through the membrane by evaporation at the warm air-water interface on the feed side followed by condensation at the cool air-water interface on the distillate side. Non-volatile solutes such as ions and metals are efficiently concentrated in the feed because they cannot transport across the membrane.[2, 4] Thus, non-volatile contaminants such as inorganic salts, ionic species, metals, and pathogenic micro-organisms typically exhibit near 100% rejection during MD, implying potential applications for water or wastewater treatment. [5-6 7-8]

9

When considering applications such as wastewater treatment and water reuse, the capabilities of MD separation remain unclear because such complex feed streams typically contain many semi-volatile and volatile solutes, and such solutes would be expected to transport through the MD membrane. For solutes with some volatility, separation performance will be characterized by partial rejection, and would be expected to scale with volatility. Indeed, concentration enhancement in the distillate for those constituents that are more volatile than water is even possible and would have substantial performance implications for highly volatile toxic or hazardous pollutants.[9] Wijekoon[10] and Xie[11] have shown that wastewater derived trace organic compounds (TrOCs) such as pharmaceuticals, steroid hormones, phytoestrogens, and pesticides with pK_H >9 (Henry's Law constants; $pK_H[atm \cdot m^3/mol]$ where $pK_H = -\log K_H$), all classified as non-volatile, have removal efficiency >80% during MD, with most observed removals near 100%. While promising, these results characterized performance for a relatively small subset of the constituents of concern expected in impaired water resources.

Organic solutes can be classified as non-volatile (NV), semi-volatile (SV), and volatile (V) to better understand and predict treatment performance during DCMD. With respect to volatility and Henry's law constants, typically evaluated at 25°C, NV contaminants are considered to have pK_H >6.52, SV with 5<pK_H<6.52, and V with pK_H <5.[12] Estimating permeate flux $[kg/m^2 \cdot h]$ of solutes during MD might also be useful as a tool to understand comparative transport and mass transfer processes. For instance, low volatility constituents have very little permeate flux because of their low vapor pressures, while higher permeate flux would be expected for more volatile compounds due to their higher vapor pressures. Typically, interactions between organic constituents and the membrane were assumed to not strongly affect transport because of the thousand-fold size difference between angstrom-sized molecules and the micron-sized MD

membrane pore sizes, although complex chemical conditions at air water interfaces complicate predictive capabilities. Permeate flux can be estimated by physiochemical properties such as mass diffusivities, partial vapor pressures, and mass transfer coefficients, which may allow the prediction of mass transport for water and wastewater contaminants in DCMD systems.

To assess separation performances for complex feed mixtures of water pollutants with varying chemical characteristics, we evaluated the fate of water or wastewater derived non-volatile, semi-volatile, and volatile organic contaminants in a bench scale DCMD system. Many regulated contaminants of interest to water or wastewater treatment, potential applications for waste heat driven DCMD, include those that are carcinogenic, highly mobile, toxic or aesthetically unpleasant, and are somewhat volatile.[13-15] Therefore, analytes evaluated in our system included PPCPs, nitrosamines, and a suite of regulated organic contaminants.[16] We included PPCPs such as caffeine and carbamazepine because they are detected frequently in municipal wastewater effluents and represent organic micropollutant classes typically used to evaluate the performance of advanced wastewater treatment processes.[17-19] With system data, we correlated observed rejections with chemical parameters such as Henry's law constants, enthalpy of vaporization, and dissociation constants. The sensitivity of Henry's law constants and vapor pressure to temperature was also evaluated. While MD performance for non- or low volatility wastewater-derived contaminants has been explored, MD performance for complex mixtures consisting of wastewater-derived contaminants with diverse higher volatility characteristics has not been explored.[20] Therefore, this study was evaluated treatment performances for volatiles to non-volatile pollutants and investigated physiochemical parameters influenced on their performances. This assessment is intended to evaluate the potential use of DCMD for water quality improvement of volatile and semi-volatile contaminants by DCMD.

Chapter 2. Material and methods

2.1 DCMD system setup

A bench scale DCMD system was used to evaluate treatment performances for the targeted analytes. The system used a hydrophobic microporous polytetrafluoroethylene (PTFE) membrane module (GE Osmonics, Minnetonka, MN), with a single PTFE active layer in the membrane thickness of 67μm with a nominal pore size of 0.18μm and porosity of 80.1%.[21] The DCMD system (Figure 1) consists of a membrane cell, two low-pressure stainless steel gear drive pumps (Cole-Palmer, USA), four thermocouples, two Kynar® gas sampling bags (Analytical Specialties Inc, IL), a hot water bath (Thermo-Fisher Scientific, USA), a balance (A&D Weighing, USA), a recirculating chiller, and a heat exchanger (Thermo-Fisher Scientific, USA).[22] The membrane module measures 155mm x 92mm x 3mm with an effective surface contact area of 143cm^2. Notably, special care was taken to design a system gas-tight to minimize possible losses of volatile analytes via volatilization. Stainless steel tubing was also used to minimize adsorption to system components if possible. The feed stream was circulated at 1L/min inside the membrane cell and maintained 50° C by the hot water bath. The distillate stream was also circulated at 1L/min and kept 25° C using a recirculating chiller combined with a heat exchanger. Temperatures in feed and distillate inlets were monitored by four thermocouples and recorded by a computer connected to LabView (Version 14.0.1.4008, National Instruments, Austin Texas, USA). Two gas tight sample bags were installed in membrane cells at feed and distillate inlets and connected to two stainless steel sampling valves to collect samples from feed and distillate reservoirs. (et al Salls)

2.2 Experimental protocol

2.2.1 Semi-volatile and volatile organics

A pre-made commercial standard (the 8270 "Megamix" standard, Restek, Bellefonte, PA) of 76 volatile and semi-volatile chemicals was used to spike the bench scale DCMD system. All of the chemicals in this standard are regulated or toxic pollutants of water, and they all are amenable to analysis by EPA method 8270D. As this standard was dissolved in dichloromethane (DCM), which is immiscible in water, the standard was first sonicated (5 min), then 15 mL of methanol was added as a co-solvent. This DCM-methanol mixture was then added to a 4 L of ultrapure water in a pre-cleaned amber glass bottle and equilibrated, with mixing, for 24 hours at 4 °C, prior to addition to the DCMD feed reservoir.

Samples from the DCMD system were collected in 1-L amber glass containers, without headspace, chilled to 4 °C, spiked with deuterated standards, and solid-phase extracted (SPE) using EPA Method 525.3 with DVB Speedisks (JT Baker). The SPE disks were shipped overnight on ice to the Center for Urban Waters (Tacoma, WA) for analysis. Briefly, semi-volatile organics were eluted from the SPE disks using ~10 mL acetone and methylene chloride. The extracts were analyzed with gas chromatography-mass spectrometry using EPA method 8270D by the City of Tacoma Environmental Services Laboratory, which is a Washington State Department of Ecology accredited laboratory facility. Method reporting levels ranged from 1-10 µg/L, depending on the analyte and volume extracted. Quality assurance-quality control samples included method blanks and laboratory blank spikes, and all data used in this study passed QA/QC criteria. The experiment was conducted twice (08/24/15 - 08/26/15; 01/02/16 – 01/04/16).

2.2.2 Pharmaceuticals and Personal Care Products (PPCPs)

DCMD system performance was also evaluated for a suite of wastewater-derived PPCPs using analytical methods adapted from Keil and Neibauer (2009) and Vanderford et al. (2003). A mixture of 30 PPCPs, mostly polar and recalcitrant compounds, dissolved in water was spiked into 4 L of ultrapure water in a pre-cleaned amber glass bottle and equilibrated for 24 hours (4 °C) prior to addition. Samples were collected and shipped on ice to the Center for Urban Waters (Tacoma, WA) for analysis. Prior to extraction, isotopically-labeled surrogate compounds in methanol were added (nominal concentrations 10-250 μg/L), then samples were sequentially vacuum-filtered through 0.7 µm glass fiber filter, 0.45 and 0.2 µm PEM filter. The pH was then adjusted to 8 ± 0.1 with 0.12 M hydrochloric acid or 0.19 M sodium hydroxide. Briefly, samples were SPE extracted under vacuum at ~10 mL/min with pre-conditioned Oasis HLB cartridges (500 mg, Waters Corp.). Cartridges were dried under ultra-high purity nitrogen gas, then eluted with 5 mL 10:90 methanol:MTBE (v:v) followed by 5 mL methanol. The eluant was concentrated to 75 µL with ultra-high purity nitrogen gas in a 35°C water bath and transferred to a HPLC vial, with 1.425 mL of pH = 2.8 acetic acid and 10 µL of isotopically-labeled internal standard solution.

Extracts were analyzed by high performance liquid chromatography-tandem mass spectrometry, with a triple quadrupole mass analyzer (HPLC-MS/MS; Agilent 1290 HPLC, Agilent 6460 triple quadrupole MS) using multiple reaction monitoring (MRM) and positive/negative polarity switching. The HPLC column was an Agilent Zorbax Eclipse, 2.1 x 150 mm, dp= 3.5 µm. The injection volume was 20-100 µL; column temperature was 50°C. The mobile phase was (A) pH = 2.8 acetic acid, and (B) 100% methanol. The mobile phase flow rate was 0.4 mL/min. The mobile phase gradient was: 95% A (t = 0 to 2 min); 95% A to 60% A (t = 2 to 6 min); 60% A (t = 6 to 13 min); 60% A to 10% A (t = 13 to 18 min); 10% A (t = 18 to 22.5 min); 10% A to 95% A (t = 22.5 to 22.6 min); and 95% A (t = 22.6 to 27.5 min). The concentration of each

analyte was determined by isotope-dilution mass spectrometry and corrected based on recovery of isotopically-labeled recovery surrogates.[23]

2.2.3 Nitrosamines

Eight nitrosamines were selected as analytes: nitrosomorpholine, nitrosopyrrolidine, nitrosopiperidine, nitrosodimethylamine, nitrosomethylethylamine, nitrosodiethylamine, nitrosodipropylamine, and nitrosobutylamine. They were analyzed by EPA 8270 method, and dosed to the system with Appendix IX nitrosamine mix (Supelco, Bellefonte, PA.). One 1mL spike mixture ampule holding 2000 μg of each nitrosamine was sonicated for 5 minutes, then added to an amber glass bottle containing 4L ultrapure water at 5°C. The solution was equilibrated for 24 hours at 4 °C after addition, with mixing, then added to 14L of ultrapure water in the Kynar® bag on the feed inlet. The initial feed and distillate volume were 18L and 3L respectively, with total system volume of 21L. Feed and distillate samples (500mL) were collected every 8 hours over 48 hours, then solid phase extracted (activated charcoal SPE, Restek 521 cartridges). Samples were analyzed using gas chromatography-tandem mass spectrometry (Varian 4000 Ion Trap GC-MS/MS; positive chemical ionization with methanol, DB624 column, 30 m, 0.25 mm, 1.4 μm) and isotope dilution analytical methods.[24]

Chapter 3. Results and discussion

3.1 Mass recovery

Pollutant fate in the DCMD system was first evaluated by estimating mass recovery for the compounds added to the system. Mass recoveries of solutes were determined by mass balances which estimated with volumetric and concentration data for each consecutive time measurement:

$$M_T = (C_f \times V_f) + (C_d \times V_d) + M_{loss} \qquad (1)$$

In Eq. (1), C_f and C_d are concentrations in the feed and distillate, respectively. V_f and V_d refer to the volume in feed and distillate, respectively. M_T and M_{loss} refer to the total mass balances and mass loss which was estimated by difference. Mass recoveries of each compound during MD at given time were calculated as:

$$\text{Mass recovery } [\%]_{t=i} = \frac{(M_T)_{t=i}}{(M_T)_{t=0}} \times 100 \qquad (2)$$

Mass recoveries of 65 V, SV, and NV solutes during MD were calculated (Table 1). Eleven out of 76 compounds spiked to the system exhibited low recovery, had analytical issues or failed to pass QA/QC criteria, thus they were not considered further in this analysis. The 65 remaining compounds were classified into "good recovery" and "poor recovery" groups in Figure 2. The recoveries exceeding 60% were best characterized by log K_{ow} value < 3, suggesting more polar compounds with less affinity for hydrophobic sorption to system components (Figure 3). The compounds, divided into 9 chemical groups, were organized by their observed recoveries: good recovery group >60% (phenols, halogenated phenols, and anilines), intermediate recovery within the group (some compounds above and some below 60%; phthalate, halogenated organic, alcohol/ether, and benzidines/aromatic amines), and poor recovery <60% (halogenated benzene and PAHs). Mass recoveries of compounds within the same chemical groups were generally consistent, except for phthalates and halogenated organics which were more variable. A couple of compounds, phenols and anilines, exhibited occasional recovery up to 157% which likely resulted from analytical uncertainty.

Good recoveries for nitrosamines and PPCPs, a polar and soluble class of contaminants common to wastewater effluent,[25] were typical (Table 3), with values are mostly above 60% except sulfathiazole, which exhibited 26% recovery and was not included in subsequent analysis. We did

16

observe that 20 out of 23 PPCPs and 3 out of 8 nitrosamines exhibited recoveries of over 100%, and up to 250% in one case, during the run. While we are somewhat uncertain of the explanation for this observation, we believe that some concentration dependent analytical effects (matrix enhancement of ionization, etc) were occurring for these particular analytes in the feed as it concentrated over time, thus systematically overestimating their concentrations. Because these compounds were mostly NV, often with very low concentrations detected in the distillate, we do not believe that this analytical uncertainty much affected our data interpretation.

Solutes with low recoveries, italicized in Table 1 and Table 3, indicate mass loss of solutes in the system, including sorption to the membrane tubing surfaces, the feed and distillate reservoirs, volatilization into the limited head space in the system, or reaction. Among the possibilities explaining low recovery, sorption is likely the most plausible mechanism (Figure 2 and 3) for the more hydrophobic compounds such as halogenated benzenes and PAHs (log K_{ow} >4) that were much more likely to demonstrate low recovery (0-22% recovery). Lost mass is most likely sorbed to the hydrophobic MD membrane tubing or gas tight reservoirs, especially on the feed components.[26-27] Solvent rinses (methanol) performed after the experiment was complete were able to recover many of these hydrophobic analytes from tubing and the membrane. Hydrophilic compounds with log K_{ow} < 3 exhibited good mass recoveries (>60%) during MD process, but additional factors do affect recovery: 4-chloro-3-methylphenol (high recovery of 108% with log K_{ow} = 3.1) and naphthalene (low recovery of 28% with log K_{ow} = 3.3) have similar log K_{ow} values but very different observed recoveries. All compounds with observed recovery less than 60% were not included in subsequent data analysis.

3.2 Rejection and treatment performance

3.2.1 Calculations

Rejection (R_i) of a solute in a membrane process, indicating an inability to pass across a membrane barrier, is typically defined as [28]:

$$R_i(t) = \left(1 - \frac{C_d}{C_f}\right)(t) \times 100 \tag{3}$$

C_f and C_d are concentrations [mg/L] in the feed and distillate, respectively in Eq (3). Rejection calculations were done for each time interval when samples were collected. Likely due to dynamic equilibrium conditions in a batch system, Figure 4 shows examples from two chemical classes whose observed rejection R varied with time: (e.g. phenols and anilines). For certain compounds, (e.g. 4-nitrophenol and 4-nitroaniline), rejections are near consistent with time. For other compounds, (e.g. 2-nitrophenol and 3-methylphenol), rejections were not constant with time, and consistently decreased as the experiment progressed. This trend was most, although not always, apparent for more volatile compounds whose rejections were well below 100%, probably due to changes in the driving force for mass transfer (system concentration gradients) over time.[29] As solutes left the feed side, crossed the membrane and built up in the distillate, some "reverse" transport from the distillate back to the feed side would be expected. As system equilibrium requires many such forward-reverse transport cycles, kinetic and mass transfer limitations might best explain observed trends with time for such solutes. Also, as feed volumes decreased, the constant pumping rate (1 L/min) provided solutes in the feed more "membrane contact time" later in the experiment, potentially increasing mass transfer efficiency. These effects likely contributed to changing solute fluxes into the distillate over time. Thus, complex, non-equilibrium dynamic conditions are expected for batch DCMD systems, with mass transfer conditions varying across the different solute chemical characteristics, as well as through time. These dynamics also imply some limitations when equation (3) is used for batch systems because it does not explicitly include

18

a time component, especially as compounds get more volatile and mass transport mechanisms become more sensitive to experimental conditions. Inconsistent transport rates between feed and distillate sides likely arose from mass transfer limitations of molecular diffusion processes through liquid and air films at the interface.[30-32] Equation (3) thus represents an estimate of "overall rejection" in the system, one that compares concentration differences in the feed and distillate solutions to estimate performance and is most suitable for steady state and continuous processes.

3.2.2 Comparison with modeled rejection

To address some of the limitations of equation (3) for a batch system where time dependent behaviors were observed, we also estimated system rejections by comparing observed concentration over time for the feed and distillate solutions to predicted concentrations derived theoretically. Modeled rejection in the system can be estimated by least square curve fitting to an optimum rejection model fit by minimizing residuals (e.g. the difference concentrations estimated by rejection model fits). Solutions for a "modeled" rejection, ranging from positive to negative, are represented in Figure 5. For non-volatile solutes, when relative concentrations in the feed increase rapidly over time, rejection of a solute is likely close to 100%. For more volatile compounds, those with rejection down to 0%, or even negative rejections, their concentrations increase far more slowly in the feed with concurrent increases in the distillate. The rejection can even be highly negative (e.g. up to -320 for 2,4,6-trichlorophenol), which is explained by higher solute flux through the membrane relative to water, driving rapid decreases over time for feed concentrations.[33]

3.2.3 Rejection as a function of solute volatility

Examples of high, intermediate, and low rejection, as estimated by least square modeling, are presented (Figures 6-8). High rejection of 4-nitroaniline, a NV solute ($pK_H = 8.9$), illustrates near complete rejection (98% rejection via modeled rejection) with a clear and consistent concentration increase in feed, and near non-detect concentration in distillate (Figure 6). As an example of intermediate rejection, benzyl alcohol as a SV solute ($pK_H = 6.47$) was observed at different rejections in feed (51%) and permeate (73%) and near constant concentration in feed over time (Figure 7). 3-methylphenol and 4-methylphenol, ($pK_H = 6.1$ and 6.06, respectively) which can easily travel through the DCMD membrane due to their volatility, are quickly detected in the distillate, consistent with its concentration trends (Figure 8). This data modeling method can more accurately account for trends in feed and distillate with time in a batch system by aligning experimental data to those rejection model fits which are most consistent with theoretical expectations (Figure 5). While the advantage of this approach is that it is possible to independently estimate feed and distillate rejection as a function of time, there do exist cases where model fits for feed and distillate rejections substantially diverge, implying some uncertainly and error with the method. In some cases, these differences arise from analytical uncertainty or near non-detect concentration data, yet explanations for other cases are less certain. In particular, we were not sure whether such uncertainty is random or are biased by kinetic or hydraulic limitations to mass transfer apparent within the system. Divergence in estimates for feed and distillate rejection, most evident for more volatile solutes and those most sensitive to temperature,[34] may be an artifact derived from non-equilibrium conditions in the system.

Feed and distillate rejection via model fitting as well as overall rejection by equation (3), using data at the final time, 48 hrs, were estimated and compared (Table 3). Overall rejection was often close to an average of the observed feed and distillate model rejections; solutes with high

rejections typically are very consistent between the different approaches (Table 2). Eighteen compounds fall within a 10% difference between overall rejection and model rejection. Also of note, the model rejections from the modeled feed data are often more reliable and consistent in comparison with estimates from distillate data, where less volatile compounds are detected at low concentrations and with more uncertainty. For example, 19 compounds have feed rejections closest to overall rejections, versus 9 compounds where distillate rejections are closest to overall rejections.

Rejection for nitrosamines with varying volatility ranged from negative to positive and were well correlated to their Henry's constant from 4.25 (volatile) to 7.0 (non-volatile; see Table 3). Polar functional groups were well correlated to high rejections and Henry's constants at 50°C. Chemical structures for each compound (Figure 10) indicate that highly soluble NPYR and NMOR are non-volatile while less soluble NDBA is more volatile.[38] Rejections for polar PPCPs that are non-volatile also were well correlated to pK_H (Figure 12) with mostly high rejections observed, excluding a couple of solutes like propazine and cotenine. Due to what we think is matrix dependent analytical bias for the PPCP run, feed rejections (along with recoveries) frequently exceeded 100%. For example, carbamazepine was detected at 10.7 mg/L (140% rejection) in feed, without detection in the distillate. Because very little mass was detected in distillate for these compounds during MD, we are confident in our assessment of their DCMD performance, despite some of the analytical uncertainties. The high rejections for pharmaceuticals indicate that we can expect relatively effective treatment for these compounds during DCMD.

3.2.4 Rejection and dissociation constants

Observed rejection values are most consistent and near 100% for NV compounds with pK_H ≥9 (see Figure 9). As volatility increases, solute rejections are less often consistent with

expectations from pK_H, with lower rejection and more variability observed.[11] For example, 2-methyl-4,6-dinitrophenol (pK_H= 5.85) has an observed rejection of 90% while a similarly volatile compound 2-methylphenol (pK_H= 5.92) exhibits substantially negative rejection around -45%. This example indicates that pH also affects solute transport for ionizable compounds. In the case of 2-methyl-4,6-dinitrophenol where the system pH was above the pK_a for 4.31, most solute mass was ionized and thus non-volatile, resulting in relatively high rejection (90%) for this semi-volatile solute. For 2-methylphenol, largely un-ionized, mass transfer across the membrane was easier, with -45% rejection (Figure 9). Removal efficiencies were notably influenced by solution pH and dissociation constants were key parameters to explain differential rejection for ionizable compounds with similar volatility.[35-36] Percentage ionization for solutes is defined by[37]:

$$\% \text{ ionization} = [\text{ionized} / (\text{ionized} + \text{neutral})] \times 100\% \qquad (4)$$

Phenols were ionized when pH was higher than their pK_a values while amines were typically neutral under the same conditions (Figure 11). Despite their substantial fraction of mass in the ionized form, compounds such as 2,4,5- and 2,4,6-trichlorophenol (pK_a 7.1 and 6.2, respectively) had some of the lowest rejections observed in this study (rejections below -100 %). Because they were apparently transported through membranes very effectively under the circumneutral pH conditions of the system, despite the fact that they were not the most volatile solutes, acid base dissociation kinetics did not seem to limit the kinetics of mass transfer through the DCMD membrane. The neutral amines, including 2-, 3-, and 4-nitroaniline (pK_a -0.28, 2.47, and 1.0) concentrated in the feed because of their low volatility (pK_H 7.23, 8.1, and 8.9), with some partial transport (~70% rejection) observed for 2-nitroaniline. For neutral (un-ionized) solutes like aniline and pyridine (pK_H= 5.69 and 4.96, respectively), the influence of pH was less clear, although rejections of these volatile compounds (~69%, 23%, respectively) were higher than might be

predicted by their low pK_H values. System pH should be evaluated as a factor affecting solute separation performance.

3.2.5 Rejection comparison with literature

Wijekoon et al.[10] and Xie et al.[11] also reported high removal efficiencies for trace organic compounds, including PPCPs, and other non-volatile organics during DCMD. Seven wastewater derived compounds were common to those studies and this study, allowing treatment performance to be compared directly (Figure 13). Five compounds (i.e. ametryn, caffeine, carbamazepine, ibuprofen, and sulfamethoxazole) exhibited near complete rejections both at pH 7.0 and 9.0, consistent with their low volatility ($pK_H > 6.5$) and hydrophobicity (log Kow < 3.0). For ionizable compounds, their treatment performance might need additional studies to evaluate performance as a function of system pH. For example, sulfamethoxazole is ionized at acidic pH values (i.e. pH 3.5, 4.5, and 5.5) and ibuprofen was negatively charged at pH of 8.0 as comparison to carbamazepine's neutrality across pH 3.5 to 7.5.[36, 39] Pentachlorophenol and atrazine had lower rejections, consistent with their volatility.

3.3 Temperature dependence for chemical parameters

3.3.1 Henry's constants

For any particular solute, the sensitivity of volatility to temperature should impact expected treatment performance during DCMD. Figure 9 also plots the temperature dependence of Henry's constants at our feed and distillate temperatures (T_f and T_d) of 25°C and 50°C, respectively. Henry's constants at T_f (50°C) were corrected by Van't Hoff equation and differences between 25°C and 50°C were shown by logarithmic values, $p(\Delta K_H) = -\log(K_{H,50°C} - K_{H,25°C})$. Some papers[10, 40, 41] noted pK_H variations likely impact rejection after correction to T_f (50–70 °C).

23

Likewise, solute volatilities have different sensitivity to temperature (derived from their enthalpy of vaporization) that translates to different performance expectations for rejection. The difference in volatility at feed and distillate temperatures can be expressed as a ΔK_H gap (Figure 14). Larger differences in ΔK_H, likely imply lower distillate to feed transport potential and increased probability of non-equilibrium conditions for any specific solute. The enthalpy of vaporization includes intermolecular forces by van der Waals forces, hydrogen bonding, and molecular surface tension, all factors impacting solute transport.[42] As typical for non-volatile compounds, PPCP groups were less sensitive to temperature with p(ΔK_H) of 6 to 17 for the T_f and T_d.[36] For those NV solutes which were most sensitive to temperature, based on their corrected pK_H values at 50°C, more transport than might be expected initially by observation of their Henry's constants at 25°C was evident. Moderate rejections (i.e. 35% to 69%) were observed by several NVs (i.e. dimethyl phthalate, 2-nitroaniline, 2,4-dinitrotoluene, 2,4,6-tribromophenol, and pentachlorophenol) despite their classifications as NV based on their 25°C pK_H values. However, their corrected pK_H values at T_f, 50°C were lower or near 6.52, close to SV classification. The pK_H values can increase even more substantially at higher enthalpies of vaporization and larger temperature differences in feed and distillate solutions. For example, if modifying the T_f in MD to 70°C, the pK_H value for 3-nitroaniline (overall R = 94%) would decrease to 6.84, which is similar with pentachlorophenol (i.e. pK_H 6.83) that was observed at 39% rejection at T_f, 50°C. Therefore, prediction of treatment performances for contaminants based on their pK_H value should start by first correcting their pK_H value to T_f for the DCMD system of interest.

3.3.2 Vapor pressures

Vapor pressures for solutes also depended on temperature differences in feed and distillate. Antoine equation and Grain Watson method were used to correct vapor pressures to T_f. Solutes with bigger vapor pressure differences across the membranes, slowing distillate to feed transport, likely resulted in non-equilibrium conditions for these solutes. This effects may have contributed to observed rejection gaps (ΔR_i), or the difference between data modeled rejections based upon feed and distillate concentrations (Figure 5). At high vapor pressures, solutes only require less energy for vaporization.[43-44] Therefore, V and SV solutes easily increased their mass transport across membranes from feed to distillate.

Inverse correlation of enthalpy of vaporization (ΔH_{vap}) and vapor pressure differences (Δp) were consistent with ΔR_i values except for two solutes: N-nitrosopiperidine (NPIP) and N-nitrosomethylethylamine (NMEA, see Figure 15). NPIP and NMEA were greatly deviated from the correlation of overall rejection to Henry's constant at 50°C (Figure 10). Thus, for any specific solute, the inter-relationships between Henry's constants, vapor pressures, and enthalpy of vaporization likely governs volatility, equilibrium, and mass transfer for solutes in DCMD systems.

3.4 Contaminant mass flux and transport

3.4.1 Mass flux of contaminants

Permeate flux is usually described in literature as a mean of evaluating the overall transport of solutes from the feed to the distillate, especially while evaluating whether the flux is stable over time as an aspect of membrane performance.[10-11, 40] Typically, permeate fluxes of solutes such as wastewater contaminants are not evaluated because most compounds separated by MD systems are non-volatile and expected to concentrate in the feed. However, given the range of solute

characteristics in our experiment, including V and SV solutes, a wide range of negative to positive rejection outcomes is evident. We estimated permeate flux for some of our solutes by two approaches: Dusty gas model (DGM) and Fick's law. The mass transfer in boundary layers and at membrane interfaces is explained by film theory and the DGM, respectively. The DGM has been employed to analyze the permeate flux for feed solution across the membranes and includes Knudsen diffusion, molecular diffusion, surface diffusion, and viscous flow mechanism. Surface diffusion and viscous flow are generally neglected in MD. The Knudsen number defined as[1]

$$\text{Kn} = \lambda/d_p \tag{5}$$

where, λ and d_p refer to mean free path [μm] and pore diameter [μm], respectively. It determines relative diffusion rates under given experimental values. The Kn values for V, SV, and NV solutes varied from 0.1-0.3 at T_f by their collision diameters, which is a term to calculate a mean free path, λ and shown that the path length is not smaller than the membrane pore diameter. Permeability for solutes as well as water (Kn = 0.92) is in transition region (i.e. 0.01 < Kn < 10) between Knudsen and ordinary molecular diffusion mechanism.[1, 45-47] However, measured water permeate flux with the PTFE membrane under the near identical membrane properties (i.e. pore size, porosity, tortuosity, and thickness) disagreed with predicted flux considered by Knudsen-molecular diffusion.[21] The large prediction error of 32.5% indicates the need to modify the permeate flux estimation. Interestingly, the Srisurichan[45] method of prediction for permeate flux only based on molecular diffusion model was quite near to experimental permeate flux under the same T_f and tortuosity factor, τ despite of the difference using a PVDF membrane.

3.4.2 Predict mass flux of contaminants

26

Estimation of water vapor permeability across membranes is generally conducted by three models: Knudsen diffusion, molecular diffusion, and Knudsen-diffusion mechanisms. Molecular diffusion model is employed by both Fick's law and the DGM models. It contains vapor pressure differences in feed and distillate and diffusivity from Fick's law as well as considering membrane coefficient by the DGM. The molecular diffusion model likely interprets mass transfer for volatile substituents by vapor pressure differences and Henry's constants due to temperature gradient across the membranes. Collision effect to the membrane pores, Knudsen diffusion was not considered to focus on mass transport for solutes. The permeate flux [$kg/m^3 \cdot h$] by molecular diffusion is described as:

$$N_i = \frac{\varepsilon}{\tau\delta} \frac{PD_{AB}M_i}{RT} \frac{(p_F - p_D)}{p_a} \tag{6}$$

where ε is porosity [m], τ is tortuosity, and δ is membrane thickness [m]. P and D_{AB} refers to total pressure [Pa] and mass diffusivity [m^2/s]. Partial vapor pressure for solutes at feed, distillate, and partial pressure of air [Pa] refer to p_F, p_D, and p_a, respectively. A group of nitrosamines was used to correlate their predicted permeate flux and observed ΔR since they had consistent relationships between pK_H from V to NV solutes (Figure 15). Mainly, influenced by vapor pressure differences, higher permeate flux (N = 3.4 g/$m^2 \cdot h$) for NDMA results in bigger ΔR_i (i.e. 68.8%) between feed and distillate. High permeate flux may indicate slow reverse flux (i.e. distillate to feed) and increased deviated from equilibrium. NDBA predicted slower permeate flux (N = 0.1 g/$m^2 \cdot h$), and was observed with little rejection differences. The NPYR, NMOR, and NPIP observed overall positive rejections, deviated mostly from the correlation between flux and ΔR_i. The low volatility comparatively for NPYR and NMOR defined as NV enabled them to concentrate their mass on the feed and concludes in low ΔR_i. The linear correlation of observed ΔR_i and theoretical predicted

permeate flux indicate a possibility to estimate an equilibrium state of solutes via their permeability across the membranes.

3.4.3 Mass flux and resistances

Inverse correlation with the permeate flux is a resistance in the two phases, gas and liquid. The two resistance model developed by Whitman[31] enables to estimate gas transfer rates and the flux determined by molecular diffusion. Resistance in liquid phase (R_L) was analyzed because it is more affected by molecular movement in the solution than in gas phase. Volatile substituents which are less soluble are consistently decreased their mass transfer rates, influenced by R_L. The R_L is regarded as the ratio of the driving force to the rate of mass transfer and defined as[28]

$$R_L = \frac{H}{H + RT(\frac{k_L}{k_G})} \tag{7}$$

where H, R, and T mean Henry's constants [$atm \cdot m^3 / mol$], the gas constant [$atm \cdot m^3 / K \cdot mol$], and temperature [K]. Mass transfer coefficients for gas and liquid (k_G and k_L) were estimated based on mass diffusivities in each phase. The eleven approaches for diffusivities including a temperature dependence at T_f were given (Table 4) and used to calculate the R_L.[43] Calculated R_L based on the seven equations were compared with Chapra's resistance estimated in two systems: great lakes and small sheltered lakes.[30] The R_L correlated by fourth equation of diffusivity represented almost close to "small sheltered lakes system" (See Figure 16). Our experimental DCMD system was covered in stainless steel and estimated not interrupted by any other obstacles, which is similar with "the small sheltered lakes system" free from wind impacts. This system was controlled by resistances in liquid phase for the mass transfer than another system such as great lakes. The seven resistance graphs at T_d, 25°C deviates within 1-5% standard

28

deviation from pK_H, 2.41 to 4.8. The mostly diverged range (i.e. pK_H 3.2 – 4.8) is in the middle of gas and liquid controlled so expected controlled by both gas and liquid film. Temperature dependence on resistance is also shown that higher Henry's constants and mass transfer coefficients at T_f shift the resistance control to the liquid film. One note for the plot is that the R_L is estimable for mostly volatiles with $pK_H < 5$. The SV and NVs are likely predicted their resistance in gas phase due to inclined to be more gas-phase controlled. The resistance can be combined with permeate flux to determine their mass transfer in membranes: volatiles controlled by liquid phase likely transport slower in the solution while semi-volatiles and non-volatiles moderately move in gas phase due to controlled by gas phase.

Chapter 4. Conclusion

We conducted a DCMD experiment with a subset of volatile, semi-volatile and non-volatile contaminants to determine their treatment performances in relation to their physiochemical parameters. Solutes defined as non-volatile with $pK_H > 7$ at feed temperature were observed at nearly complete rejections in the DCMD system, but volatiles and semi-volatile solutes exhibited separation efficiencies from negative to positive values. Acid dissociation constant, pK_a was one parameter that clearly influenced rejections for some solutes by reducing overall solutes volatility (i.e. 2-methyl-4,6-dinitrophenol) when ionized at DCMD system conditions. Modeled rejections independently based upon feed and distillate data demonstrate a wide range of rejection outcomes for system components, from zero to – 580%, with solute transport driven by the temperature and volatility differences across the membrane. The ΔR values were inter-correlated to chemical properties and were sensitive to temperature dependence, Henry's constant, enthalpy of

vaporizations, vapor pressure difference, and permeate fluxes. The different chemical characteristics for solutes between feed and distillate membrane interfaces results in differential equilibrium and permeability through the membranes, indicating that Henry's constant K_H, the typical metric of volatility, is not always fully predictive of DCMD rejection. More detailed and accurate estimates of mass transport across the membranes derived from first principles (such as chemical potential) should be estimated from physical parameters such as mass diffusivities and mass transfer coefficients to better understand fate outcomes for solutes with some volatility attributes.

Nomenclature

C   concentration (mg/L)

d_p pore diameter (µm)

D_{AB} mass diffusivity from A to B phase(m^2/s)

K_a acid dissociation constant (dimensionless)

k_G mass transfer coefficient in gas phase (m/s)

K_H Henry's constant ($atm \cdot m^3/mol$)

k_L mass transfer coefficient in liquid phase (m/s)

Kn   Knudsen number (dimensionless)

K_{ow} Octanol-Water partition coefficient (dimensionless)

M   molecular weight (g/mol)

M_{loss} mass loss (g)

M_T total mass balance (g)

N_i permeate flux of i ($g/m^3 \cdot h$)

p partial vapor pressure (pa)

P   total pressure (pa)

R   universal gas constant ($atm \cdot m^3 / K \cdot mol$)

R_i rejection of i (%)

R_L resistance in liquid phase

t   time (min)

T   temperature (K)

V   volume (L)

Greek symbols

λ mean free path (µm)

ε   porosity (m]

τ   tortuosity (dimensionless)

δ   membrane thickness (m)

Subscripts

a   air

f   feed

d   distillate

Works Cited

1.   Khayet, M., *Membrane distillation : principles and applications*. Amersterdam ; Boston : Elsevier: Amersterdam ; Boston, 2011.

2.   Alkhudhiri, A.; Darwish, N.; Hilal, N., Membrane distillation: A comprehensive review. *Desalination* **2012,** *287*, 2-18.

3.   Martinetti, C. R.; Childress, A. E.; Cath, T. Y., High recovery of concentrated RO brines using forward osmosis and membrane distillation. *Journal of Membrane Science* **2009,** *331* (1-2), 31-39.

4.   Lawson, K. W.; Lloyd, D. R., Membrane distillation. *Journal of Membrane Science* **1997,** *124* (1), 1-25.

5.   Curcio, E.; Drioli, E., Membrane distillation and related operations - A review. *Separation and Purification Reviews* **2005,** *34* (1), 35-86.

6.   Khayet, M., Membranes and theoretical modeling of membrane distillation: A review. *Advances in Colloid and Interface Science* **2011,** *164* (1-2), 56-88.

7.   Alkhudhiri, A.; Darwish, N.; Hilal, N., Treatment of saline solutions using Air Gap Membrane Distillation: Experimental study. *Desalination* **2013,** *323*, 2-7.

8.   Cath, T. Y.; Adams, V. D.; Childress, A. E., Experimental study of desalination using direct contact membrane distillation: a new approach to flux enhancement. *Journal of Membrane Science* **2004,** *228* (1), 5-16.

9.   Tomaszewska, M., Membrane distillation - Examples of applications in technology and environmental protection. *Polish Journal of Environmental Studies* **2000,** *9* (1), 27-36.

10.   Wijekoon, K. C.; Hai, F. I.; Kang, J. G.; Price, W. E.; Cath, T. Y.; Nghiem, L. D., Rejection and fate of trace organic compounds (TrOCs) during membrane distillation. *Journal of Membrane Science* **2014,** *453*, 636-642.

11.   Xie, M.; Nghiem, L. D.; Price, W. E.; Elimelech, M., A Forward Osmosis-Membrane Distillation Hybrid Process for Direct Sewer Mining: System Performance and Limitations. *Environmental Science & Technology* **2013,** *47* (23), 13486-13493.

12.   Zhang, C., *Fundamentals of environmental sampling and analysis*. Hoboken, N.J. : Wiley-Interscience: Hoboken, N.J., 2007.

13.   Snyder, S. A., Occurrence, treatment, and toxicological relevance of EDCs and pharmaceuticals in water. *Ozone-Science & Engineering* **2008,** *30* (1), 65-69.

14.   Snyder, S. A.; Benotti, M. J., Endocrine disruptors and pharmaceuticals: implications for water sustainability. *Water Science and Technology* **2010,** *61* (1), 145-154.

15.   Chary, N. S.; Fernandez-Alba, A. R., Determination of volatile organic compounds in drinking and environmental waters. *Trends in Analytical Chemistry* **2011**.

16.   Plumlee, M. H.; Lopez-Mesas, M.; Heidlberger, A.; Ishida, K. P.; Reinhard, M., N-nitrosodimethylamine (NDMA) removal by reverse osmosis and UV treatment and analysis via LC-MS/MS. *Water Research* **2008,** *42* (1-2), 347-355.

17.   Daneshvar, A.; Aboulfadl, K.; Viglino, L.; Broseus, R.; Sauve, S.; Madoux-Humery, A. S.; Weyhenmeyer, G. A.; Prevost, M., Evaluating pharmaceuticals and caffeine as indicators of fecal contamination in drinking water sources of the Greater Montreal region. *Chemosphere* **2012,** *88* (1), 131-139.

18.   Miao, X. S.; Yang, J. J.; Metcalfe, C. D., Carbamazepine and its metabolites in wastewater and in biosolids in a municipal wastewater treatment plant. *Environmental Science & Technology* **2005,** *39* (19), 7469-7475.

19.   Carballa, M.; Omil, F.; Lema, J. M.; Llompart, M.; Garcia-Jares, C.; Rodriguez, I.; Gomez, M.; Ternes, T., Behavior of pharmaceuticals, cosmetics and hormones in a sewage treatment plant. *Water Research* **2004,** *38* (12), 2918-2926.

20.   Gryta, M.; Tomaszewska, M.; Karakulski, K., Wastewater treatment by membrane distillation. *Desalination* **2006,** *198* (1), 67-73.

21.   Rao, G.; Hiibel, S. R.; Childress, A. E., Simplified flux prediction in direct- contact membrane distillation using a membrane structural parameter. *Desalination* **2014,** *351*, 151-162.

22.   Gustafson, R. D.; Murphy, J. R.; Achilli, A., A stepwise model of direct contact membrane distillation for application to large- scale systems: Experimental results and model predictions. *Desalination* **2016,** *378*, 14-27.

23.   James, C. A.; Miller-Schulze, J. P.; Ultican, S.; Gipe, A. D.; Baker, J. E., Evaluating Contaminants of Emerging Concern as tracers of wastewater from septic systems. *Water Research* **2016,** *101*, 241-251.

24.   Holady, J. C.; Trenholm, R. A.; Snyder, S. A., Use of Automated Solid-Phase Extraction and GC-MS/MS to Evaluate Nitrosamines in Water Matrices. *American Laboratory* **2012,** *44* (3), 25-30.

25.   Snyder, S. A.; Westerhoff, P.; Yoon, Y.; Sedlak, D. L., Pharmaceuticals, Personal Care Products, and Endocrine Disruptors in Water: Implications for the Water Industry. *Environmental Engineering Science* **2003,** *20* (5), 449-469.

26.   Quantitative drug design; a critical introduction, 2d ed. Ringgold Inc: Portland, 2010; Vol. 34.

27.   Yoon, Y.; Westerhoff, P.; Snyder, S. A.; Wert, E. C.; Yoon, J., Removal of endocrine disrupting compounds and pharmaceuticals by nanofiltration and ultrafiltration membranes. *Desalination* **2007,** *202* (1), 16-23.

28.   Benjamin, M. M., *Water Quality Engineering Physical / Chemical Treatment Processes*. Hoboken : Wiley: Hoboken, 2013.

29.   Hoek, E. M. V.; Elimelech, M., Cake- enhanced concentration polarization: a new fouling mechanism for salt- rejecting membranes. *Environmental science & technology* **2003,** *37* (24), 5581.

30.   Chapra, S. C., *Surface water-quality modeling*. Long Grove, Ill. : Waveland Press: Long Grove, Ill., 2008.

31.   Whitman, W. G., The two film theory of gas absorption. *International Journal of Heat and Mass Transfer* **1962,** *5* (5), 429-433.

32.   Nghiem, L. D.; Schäfer, A. I.; Elimelech, M., Removal of natural hormones by nanofiltration membranes: measurement, modeling, and mechanisms. *Environmental science & technology* **2004,** *38* (6), 1888.

33.   Cho, C. H.; Oh, K. Y.; Kim, S. K.; Yeo, J. G.; Sharma, P., Pervaporative seawater desalination using NaA zeolite membrane: Mechanisms of high water flux and high salt rejection. *Journal of Membrane Science* **2011,** *371* (1-2), 226-238.

34.   Banat, F. A.; Simandl, J., Theoretical and experimental study in membrane distillation. *Desalination* **1994,** *95* (1), 39-52.

35.   Ozaki, H.; Li, H., Rejection of organic compounds by ultra- low pressure reverse osmosis membrane. *Water Research* **2002,** *36* (1), 123-130.

36.   Nghiem, L. D.; Schäfer, A. I.; Elimelech, M., Pharmaceutical retention mechanisms by nanofiltration membranes. *Environmental science & technology* **2005,** *39* (19), 7698.

37.   Remington, J. P.; Beringer, P., *Remington : the science and practice of pharmacy*. 21st ed. ed.; Philadelphia : Lippincott Williams & Wilkins: Philadelphia, 2006.

38.   Mitch, W.; Sharp, J.; Trussell, R.; Valentine, R.; Alvarez-Cohen, L.; Sedlak, D. L., N-nitrosodimethylamine (NDMA) as a drinking water contaminant: A review. In *Environ. Eng. Sci.*, 2003; Vol. 20, pp 389-404.

39.   Xie, M.; Price, W. E.; Nghiem, L. D., Rejection of pharmaceutically active compounds by forward osmosis: Role of solution pH and membrane orientation. *Separation and Purification Technology* **2012**, *93*, 107-114.

40.   Naidu, G.; Jeong, S.; Choi, Y.; Vigneswaran, S., Membrane distillation for wastewater reverse osmosis concentrate treatment with water reuse potential. *Journal of Membrane Science* **2017,** *524*, 565-575.

41.   Al-Obaidani, S.; Curcio, E.; Macedonio, F.; Di Profio, G.; Al-Hinai, H.; Drioli, E., Potential of membrane distillation in seawater desalination: Thermal efficiency, sensitivity study and cost estimation. *Journal of Membrane Science* **2008,** *323* (1), 85-98.

42.   Schwarzenbach, R. P., *Environmental organic chemistry*. 2nd ed. ed.; Hoboken, N.J. : Wiley: Hoboken, N.J., 2003.

43.   Zaitsau, D. H.; Kabo, G. J.; Strechan, A. A.; Paulechka, Y. U.; Tschersich, A.; Verevkin, S. P.; Heintz, A., Experimental vapor pressures of 1- alkyl- 3- methylimidazolium bis(trifluoromethylsulfonyl) imides and a correlation scheme for estimation of vaporization enthalpies of ionic liquids. *The journal of physical chemistry. A* **2006,** *110* (22), 7303.

44.   Chickos, J. S.; Hanshaw, W., Vapor Pressures and Vaporization Enthalpies of the n - Alkanes from C 21 to C 30 at T = 298.15 K by Correlation Gas Chromatography. *J. Chem. Eng. Data* **2004,** *49* (1), 77-85.

45.   Srisurichan, S.; Jiraratananon, R.; Fane, A. G., Mass transfer mechanisms and transport resistances in direct contact membrane distillation process. *Journal of Membrane Science* **2006,** *277* (1), 186-194.

46.   Alicia Kyoungjin, A.; Eui-Jong, L.; Jiaxin, G.; Sanghyun, J.; Jung-Gil, L.; Noreddine, G., Enhanced vapor transport in membrane distillation via functionalized carbon nanotubes anchored into electrospun nanofibres. *Scientific Reports* **2017,** *7*.

47.   Brodkey, R. S., *Transport phenomena : a unified approach*. New York : McGraw-Hill: New York, 1988.

48.   Fuller, E. N.; Schettler, P. D.; Giddings, J. C., NEW METHOD FOR PREDICTION OF BINARY GAS- PHASE DIFFUSION COEFFICIENTS. *Ind. Eng. Chem.* **1966,** *58* (5), 18-27.

49.   A new method for prediction of binary gas- phase diffusion coefficients.: E N Fuller et al. , Ind Eng Chem , 58 , 1966, 18–27. 1966; Vol. 16, pp 551-551.

50.   Bird, R. B., *Transport phenomena*. 2nd, Wiley international ed. ed.; New York : J. Wiley: New York, 2002.

51.   Hayduk, W.; Laudie, H., Prediction of diffusion coefficients for nonelectrolytes in dilute aqueous solutions. *AIChE Journal* **1974,** *20* (3), 611-615.

52.   Einstein, A., *Investigations on the theory of the Brownian movement*. New York : Dutton: New York, 1915.

Table 1. Observed mass recoveries [%] of 65 non-volatiles, semi-volatiles, and volatiles based on chemical group. Three categories of good (> 60%), intermediate (combined with good and poor recovery), and poor (< 60%) recovery are used to classify each group. 33 solutes with < 60% recoveries are italicized. SD [%] refers to standard deviation.

"Good recovery"	Recovery [%]	SD [%]	"Intermediate recovery"	Recovery [%]	SD [%]	"Poor recovery"	Recovery [%]	SD [%]
Phenols			**Phthalate**			**Halogenated benzene**		
2,4-Dimethylphenol	117	12	*Butyl benzyl phthalate*	14	5	*1,2,4-Trichlorobenzene*	14	30
2-Methyl-4,6-dinitrophenol	145	23	Diethylphthalate	88	17	*1,2-Dichlorobenzene*	31	25
2-Methylphenol	113	9	Dimethyl phthalate	103	21	*1,3-Dichlorobenzene*	27	26
2-Nitrophenol	115	11	*Di-n-butylphthalate*	19	6	*1,4-Dichlorobenzene*	27	26
3-Methylphenol	114	10	*Di-n-Octyl phthalate*	5	4	*Hexachlorobenzene*	4	0
4-Nitrophenol	157	27						
Phenol	85	9	**Halogenated organic**			**PAHs**		
			Hexachloroethane	22	6	*Naphthalene*	28	5
Halogenated phenols			*Hexachlorobutadiene*	4	0	*Acenaphthene*	15	30
2,4,5-Trichlorophenol	80	12	*Hexachlorocyclopentadiene*	3	0	*Acenaphthylene*	19	29
2,4,6-Tribromophenol	85	14	2-Fluorobiphenyl	78	10	*Fluorene*	12	4
2,4,6-Trichlorophenol	95	9				*Phenanthrene*	9	3
2,4-Dichlorophenol	103	9	**Alcohol/Ether**			*Anthracene*	8	2
2-Chlorophenol	110	16	Benzyl Alcohol	95	11	*Benzo(b,)fluoranthenes*	3	1
2-Fluorophenol	83	12	Bis(2chloroisopropyl) ether	98	13	*Benzo(a)anthracene*	4	1
4-Chloro-3-methylphenol	108	10	bis(2-Chloroethyl)ether	110	18	*Pyrene*	5	1
Pentachlorophenol	64	17	*4-Bromophenyl phenyl ether*	8	2	*Chrysene*	4	1
			4-Chlorophenyl phenyl ether	9	3	*Benzo(a)pyrene*	3	2
			bis(2-Chloroethoxy)methane	110	17	*Dibenz(a,h)anthracene*	3	4
Anilines						*Benzo(g,h,i)perylene*	3	3
Aniline	72	4				*Indeno(1,2,3-c,d)pyrene*	3	2
2-Nitroaniline	110	12	**Benzidines/Aromatic amines**			*2-Methylnaphthalene*	14	30
3-Nitroaniline	109	25	*1,2-Diphenylhydrazine*	20	6	*2-Chloronaphthalene*	12	31
4-Chloroaniline	91	11	Pyridine	91	7	*Fluoranthene*	4	1
4-Nitroaniline	109	14	Nitrobenzene	93	14	*Carbazole*	39	12
Other			2,4-Dinitrotoluene	82	18	*Dibenzofuran*	12	3
Isophorone	114	18	2,6-Dinitrotoluene	83	16			

Table 2. Observed rejection of 32 solutes divided into non-volatile (NV), semi-volatile (SV), and volatile (V) based on their Henry's law constants (pK_H)[12] and dissociation constants (pK_a). Feed and distillate rejection were conducted independently by least square curve fitting method as well as by an "overall rejection" calculated by equation (3). Ionizable solutes were italicized for their pK_a values.

Group	Volatility at 25C	Feed R [%]	Distillate R [%]	Overall R [%]	pKH[a] (atm*m3/mol) at 25C	pKa (% ionization) [b]
Phthalate						
Diethyl phthalate	SV	16	60	32	6.21	NA
Dimethyl phthalate	NV	64	73	67	6.71	NA
Phenols						
2-Methyl-4,6-dinitrophenol	SV	105	82	90	5.85	*4.31 (99.8%)*
Phenol	SV	-20	77	52	6.48	10.00
3-Methylphenol	SV	20	-13	-2	6.06	10.26
2-Methylphenol	SV	-13	-91	-45	5.92	10.28
2,4-Dimethylphenol	SV	-25	-188	-75	6.02	10.60
2-Nitrophenol	V	-64	-643	-120	4.89	7.23
4-Nitrophenol	NV	113	94	97	7.89	*7.15 (41.5%)*
Halogenated phenols						
2-Fluorophenol	SV	44	84	57	5.49	8.73[a]
2,4,6-Tribromophenol	NV	30	73	44	7.32	*6.80 (61.3%)*
Pentachlorophenol	NV	-20	77	38	7.61	*4.70 (99.5%)*
4-Chloro-3-methylphenol	V	25	26	14	5.61	9.55
2-Chlorophenol	V	-46	-195	-77	4.95	8.56
2,4-Dichlorophenol	SV	-68	-112	-105	5.37	7.89
2,4,5-Trichlorophenol	SV	-131	15	-120	5.66	*7.10 (44.3%)*
2,4,6-Trichlorophenol	SV	-197	-181	-320	5.38	*6.20 (86.3%)*
Aromatic amine						
4-Nitroaniline	NV	98	98	98	8.90	1.00
3-Nitroaniline	NV	94	95	94	8.10	2.47
Aniline	SV	-35	67	69	5.69	4.60
2-Nitroaniline	NV	71	72	69	7.23	-0.28
4-Chloroaniline	SV	-38	27	-32	5.51	3.98
Halogenated organic						
2-Fluorobiphenyl	V	24	78	49	3.32	NA
Alcohol/Ether						
Benzyl alcohol	SV	51	73	58	6.47	15.4[b]

Bis(2-chloroisopropyl)ether	V	-95	-121	-122	3.95	NA
Bis(2-chloroethyl)ether	V	-58	-252	-100	4.77	NA
Bis(2-chloroethoxy)methane	V	-41	-143	-81	4.95	NA
Benzidines/Aromatic amines						
Pyridine	V	13	50	23	4.96	5.23
Nitrobenzene	V	-100	-46	-90	4.62	3.98
2,4-Dinitrotoluene	NV	11	66	36	7.27	NA
2,6-Dinitrotoluene	SV	-36	42	-15	6.13	1.80
Other						
Isophorone	SV	-100	-275	-96	5.18	NA

[a]Physio-chemical data are found from Chemspider. [b]pK_a data are found from Pubchem.

Table 3. Observed recovery and rejection data and physicochemical properties of 8 nitrosamines and 23 PPCPs. Sulfathiazole italicized was not considered for subsequent analysis due to low recovery. Feed and distillate rejections (R_i) also were modeled by least square curve fittings. Overall rejection (R_i) was calculated by equation (3).

	Recovery [%]	Feed R_i [%]	Distillate R_i [%]	Overall R_i [%]	Log K_{ow}[a]	Vapor pressure[a] [mmHg] at 25°C	pK_H[a] (atm*m3/mol) at 25C
Nitrosamines							
N-Nitrosodibutylamine	65	-100.0	-100.0	-63.3	2.63	4.69E-02	4.88
N-Nitrosodipropylamine	71	-95.6	-100.0	-96.4	1.36	3.00E-01	5.27
N-Nitrosodiethylamine	83	-55.5	-100.0	-73.7	0.48	1.70E+00	5.44
N-Nitrosodimethylamine	98	-27.5	-96.3	-26.0	-0.57	4.60E+00	5.74
N-Nitrosopiperidine	118	25.7	-25.0	30.8	0.36	2.07E-01	6.07
N-Nitrosomethylethylamine	92	-65.0	-100.0	-50.7	0.04	4.10E+00	6.37
N-Nitrosopyrrolidine	247	82.8	92.9	100.0	-0.19	2.00E-01	7.31
N-Nitrosomorpholine	232	79.7	77.8	87.8	-0.44	1.34E-01	7.61
PPCPs							
Ibuproben	168	130	100	100	3.97	1.31E-07	6.82
PropylParaben	111	111	97	96	3.04	1.18E-04	8.20
EthylParaben	200	133	100	100	2.47	3.07E-04	8.32
Propazine	93	-33	97	94	2.93	8.55E-04	8.34
Carbaryl	100	47	99	99	2.36	2.74E-06	8.36
MethylParaben	209	140	95	96	1.96	2.89E-07	8.44
Nicotine	150	129	99	100	1.17	1.36E-06	8.52
Ametryn	127	106	98	97	2.98	2.21E-08	8.62
Atrazine	146	121	98	97	2.61	1.86E-04	8.63
Vanillin	141	105	96	95	1.21	9.29E-05	8.67
Simazine	157	131	99	99	2.18	3.80E-02	9.03
Mecoprop	229	143	100	100	3.20	3.00E-06	9.05
Carbamazepine	188	140	100	100	2.45	8.80E-08	9.97
Caffeine	165	131	99	100	-0.07	7.33E-09	10.45
Theobromine	132	116	100	100	-0.78	1.13E-11	10.79
Cotenine	165	-100	100	100	0.07	3.81E-04	11.48
Cyanazine	133	121	100	100	2.22	1.38E-07	11.53
Paraxanthine	80	125	100	100	-0.22	8.21E-09	11.76
Sulfamethoxazole	128	107	100	100	0.89	1.30E-07	12.02
Acetaminophen	202	154	100	100	0.46	1.94E-06	12.19
Sulfathiazole	26	-55	100	100	0.05	3.24E-08	13.23
Ensulizole	200	133	100	100	-0.16	7.32E-15	13.88
Sucralose	188	132	100	100	-1.00	3.25E-14	18.40

[a]*Physio-chemical data are found from Chemspider.*

Table 4. Computational approaches to estimate diffusivities of organic solutes in gaseous phase and liquid phase. Each equation is shown with the references.

	Gaseous Diffusion Coefficient, D_G	**Reference**	**Temperature dependence on D_G**	**Reference**
①	$D_g = \dfrac{1.55}{M^{0.65}}$	Fuller (1966) [48]	$D_{ia} = 10^{-3}\dfrac{T^{1.75}\left[(1/M_{air})+(1/M_i)\right]^{1/2}}{p\left[\bar{V}_{air}^{1/3}+\bar{V}_i^{1/3}\right]^2}$ (cm^{2}s^{-1})	Fuller, Schettler, and Giddings (1966) [49]
②	$D_{ia} = \dfrac{2.35}{(\bar{V}_i)^{0.73}}$	Schwarzenbach (2002) [42]		
③	$\dfrac{D_{ia}}{D_{ref\,a}} \approx \left[\dfrac{M_i}{M_{ref}}\right]^{-1/2}$	Schwarzenbach (2002) [42]	$\dfrac{D}{D_0} = \left[\dfrac{T}{T_0}\right]^{\frac{3}{2}}$	R. Brid, w (2001) [50]
④	$D_{ia} = 10^{-3}\dfrac{T^{1.75}\left[(1/M_{air})+(1/M_i)\right]^{1/2}}{p\left[\bar{V}_{air}^{1/3}+\bar{V}_i^{1/3}\right]^2}$ (cm^{2}s^{-1})	Fuller, Schettler, and Giddings (1966) [49]		

|	**Liquid Diffusion Coefficient, D_L**	**Reference**	**Temperature dependence on D_L**	**Reference**
①	$D_l = \dfrac{2.7\times10^{-4}}{M^{0.71}}$	Hayduk and Laudie (1974) [51]	$\dfrac{D_{T_1}}{D_{T_2}} = \dfrac{T_1}{T_2}\dfrac{\mu_{T_2}}{\mu_{T_1}}$	Einstein, A. (1905) [52]
②	$D_{iw} = \dfrac{2.3\cdot10^{-4}}{(\bar{V}_i)^{0.71}}$	Schwarzenbach (2002) [42]	$D_{AB} = 1.173\times10^{-16}\sqrt{\phi M_B}\,\dfrac{T}{\mu_B V_A^{\,0.6}}$	Christie J. Geankoplis (2003)
③	$\dfrac{D_{iw}}{D_{ref\,w}} \cong \left[\dfrac{M_i}{M_{ref}}\right]^{-1/2}$	Schwarzenbach (2002) [42]		
④	$D_{iw} = \dfrac{kT}{6\pi\eta\, r_i}$	Einstein, A (1905) [52]		
⑤	$D_{iw}\,(\text{cm}^2\text{s}^{-1}) = \dfrac{13.26\times10^{-5}}{\eta^{1.14}\bar{V}_i^{-0.589}}$	Hayduk and Laudie (1974) [51]		
⑥	$\dfrac{D_{iw}}{D_{ref\,w}} = \left[\dfrac{\bar{V}_i}{V_{ref}}\right]^{-0.589}$	Othmar and thakar 1953		
⑦	$D_{AB} = 1.173\times10^{-16}\sqrt{\phi M_B}\,\dfrac{T}{\mu_B V_A^{\,0.6}}$	Christie J. Geankoplis (2003)		
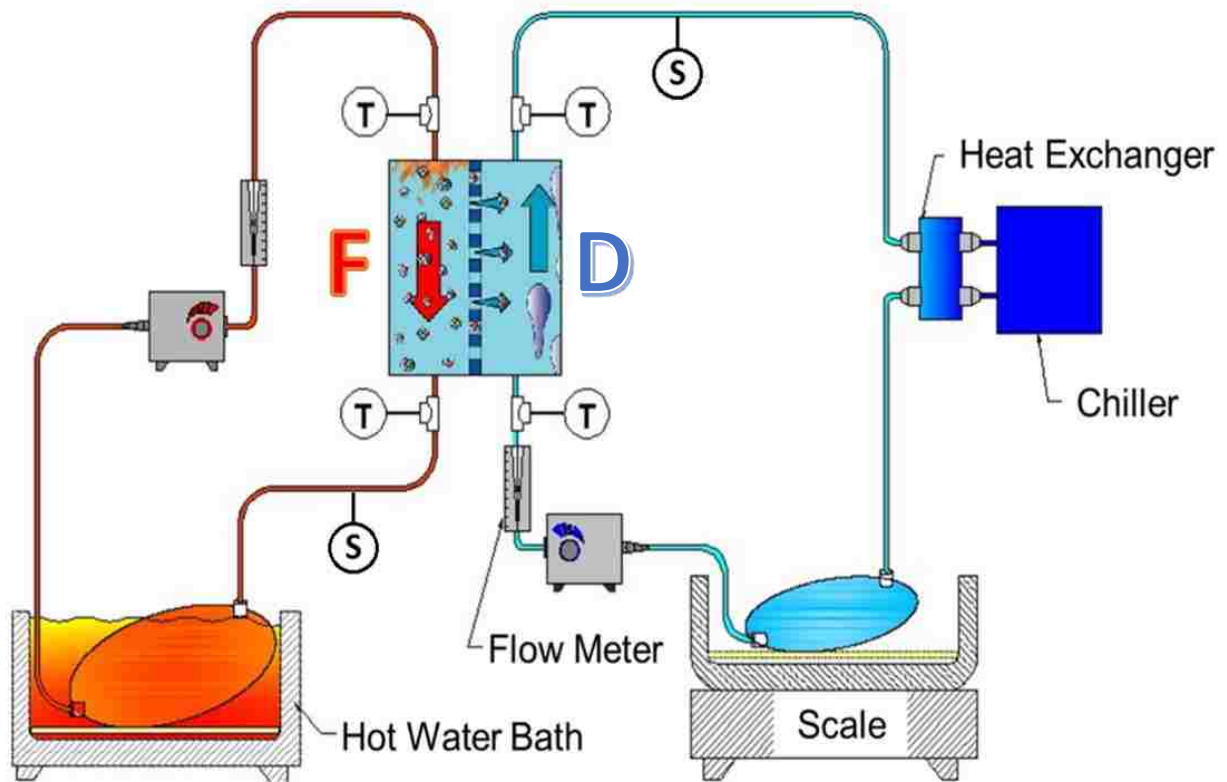
Figure 1. Schematic diagram of bench-scale DCMD system; Feed (**F**) and Distillate (**D**) as well as 4 Thermocouple (T) and 2 Sampling bags (S).
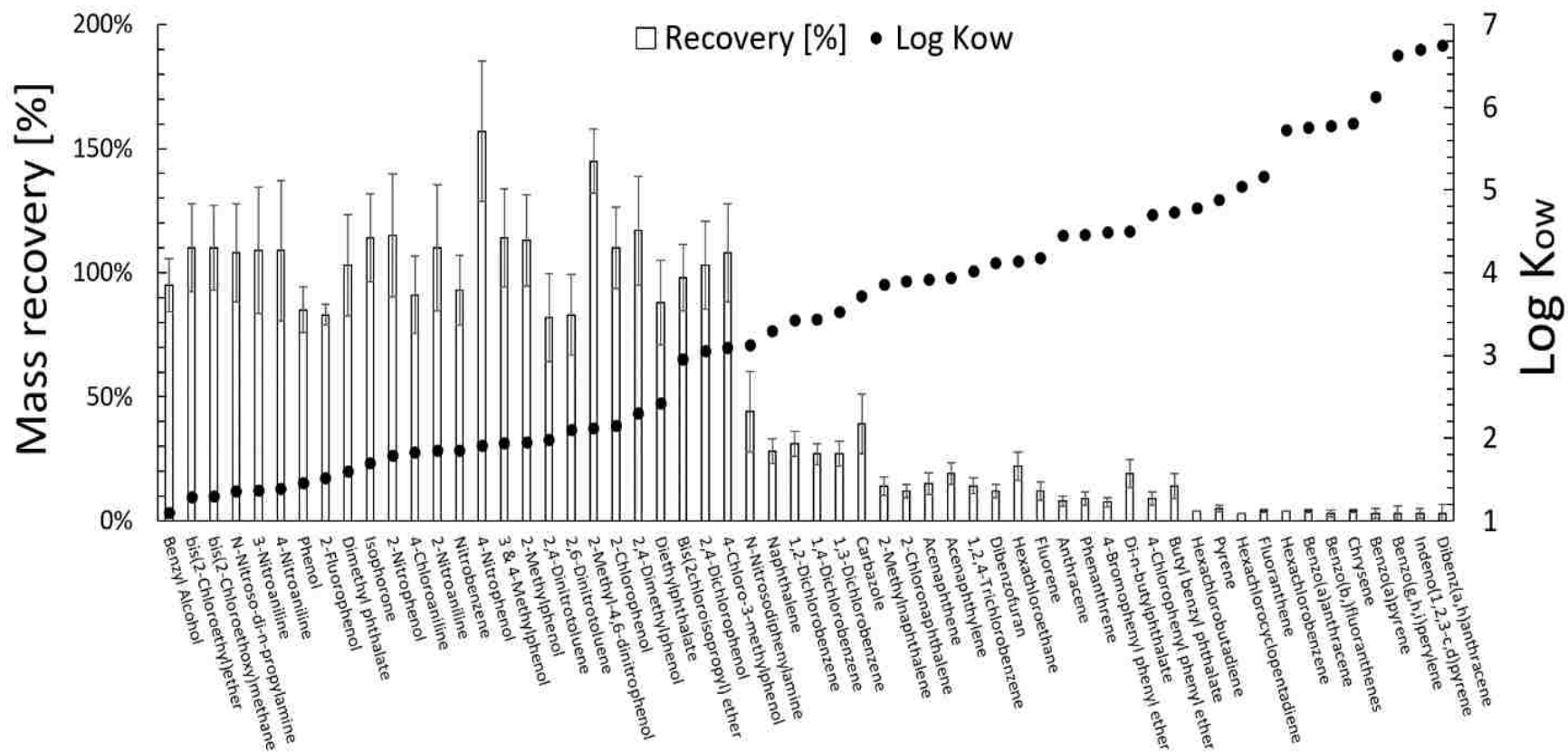
**Figure 2**. Observed mass recovery in the DCMD system. Also plotted is the log K_{ow} of organic solutes described in ascending order of log K_{ow}. Error bars represent standard deviations.
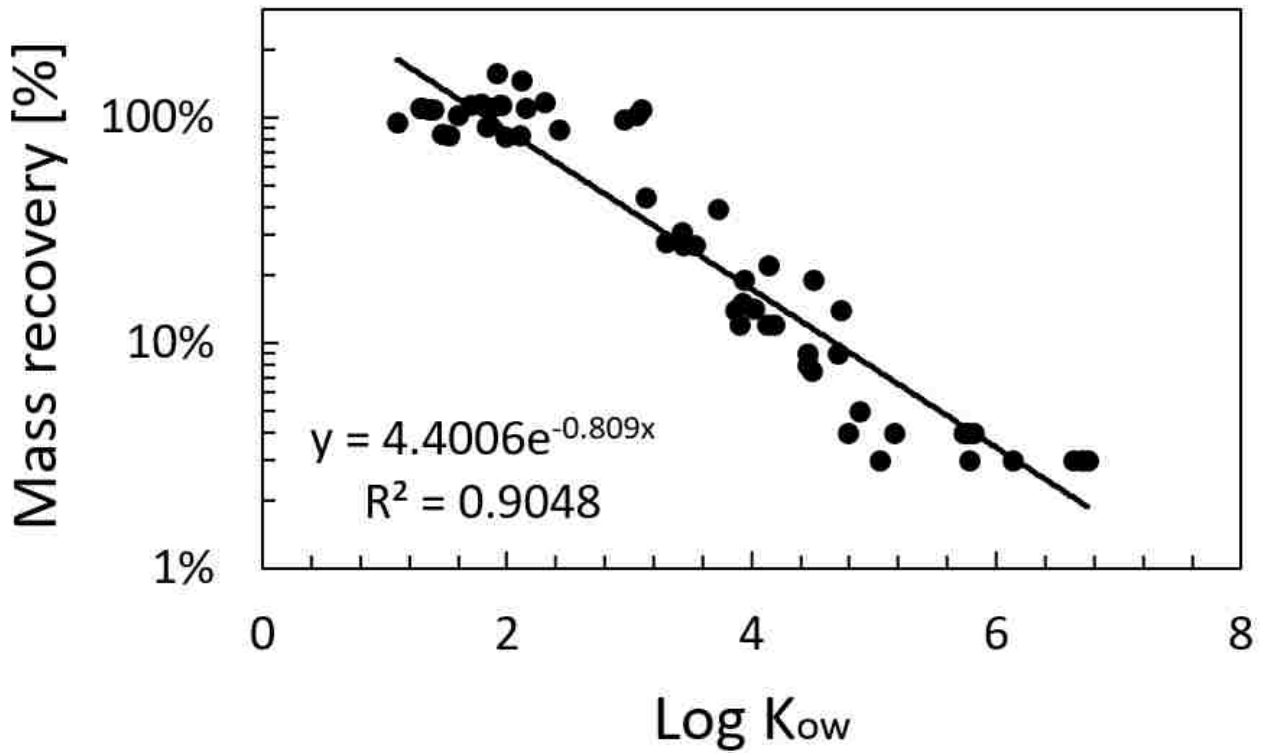
Figure 3. A correlation of observed mass recovery [%] during DCMD and octanol-water partition coefficient, log K_{ow} for semi-volatiles and volatiles, to demonstrate the relationship of hydrophobic sorption to mass loss in the system. Mass recovery is described by log-scale.
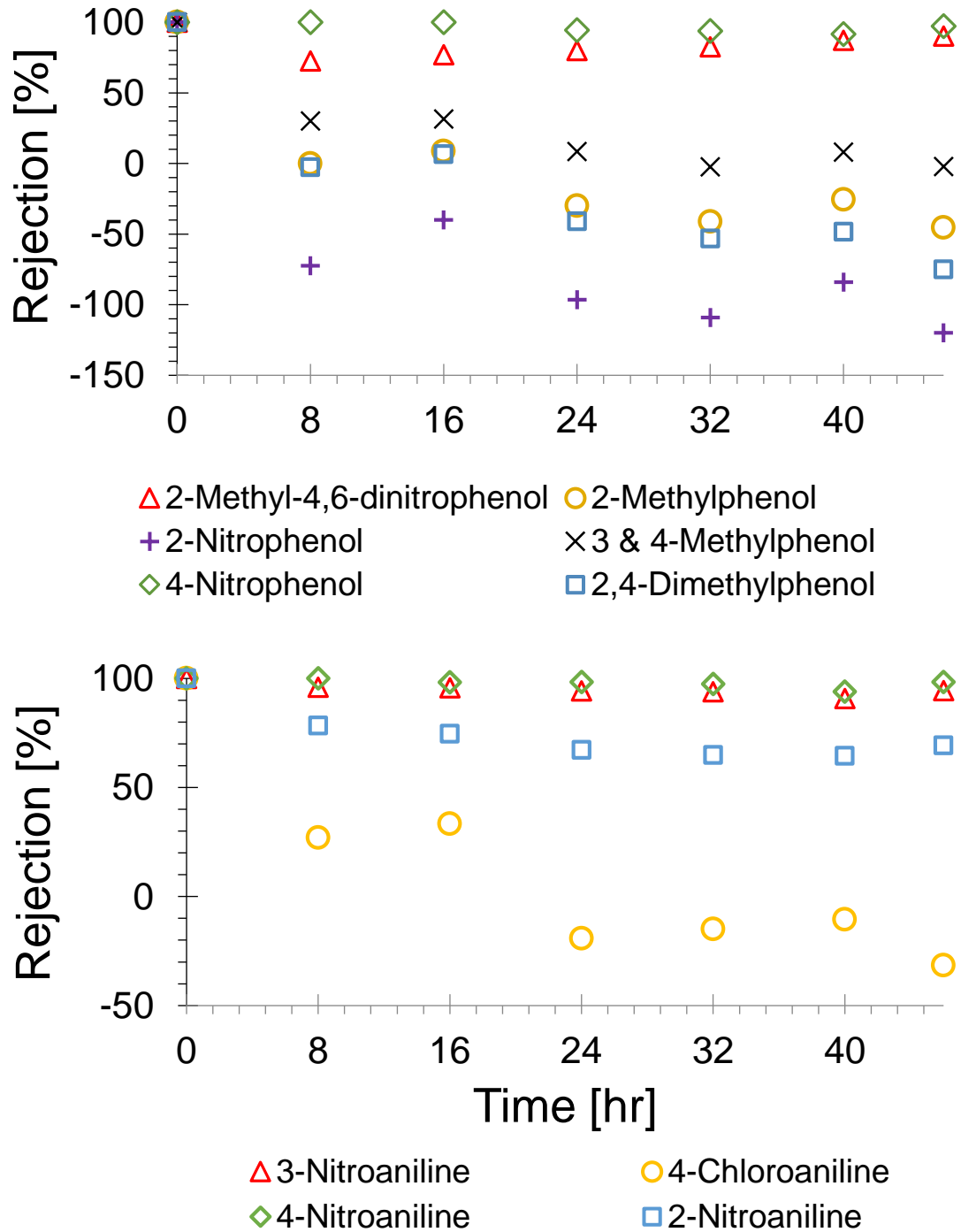
Figure 4. Observed overall rejection of phenols (A) and anilines (B) over 48 hours in the DCMD system; rejection values were calculated by equation (3).
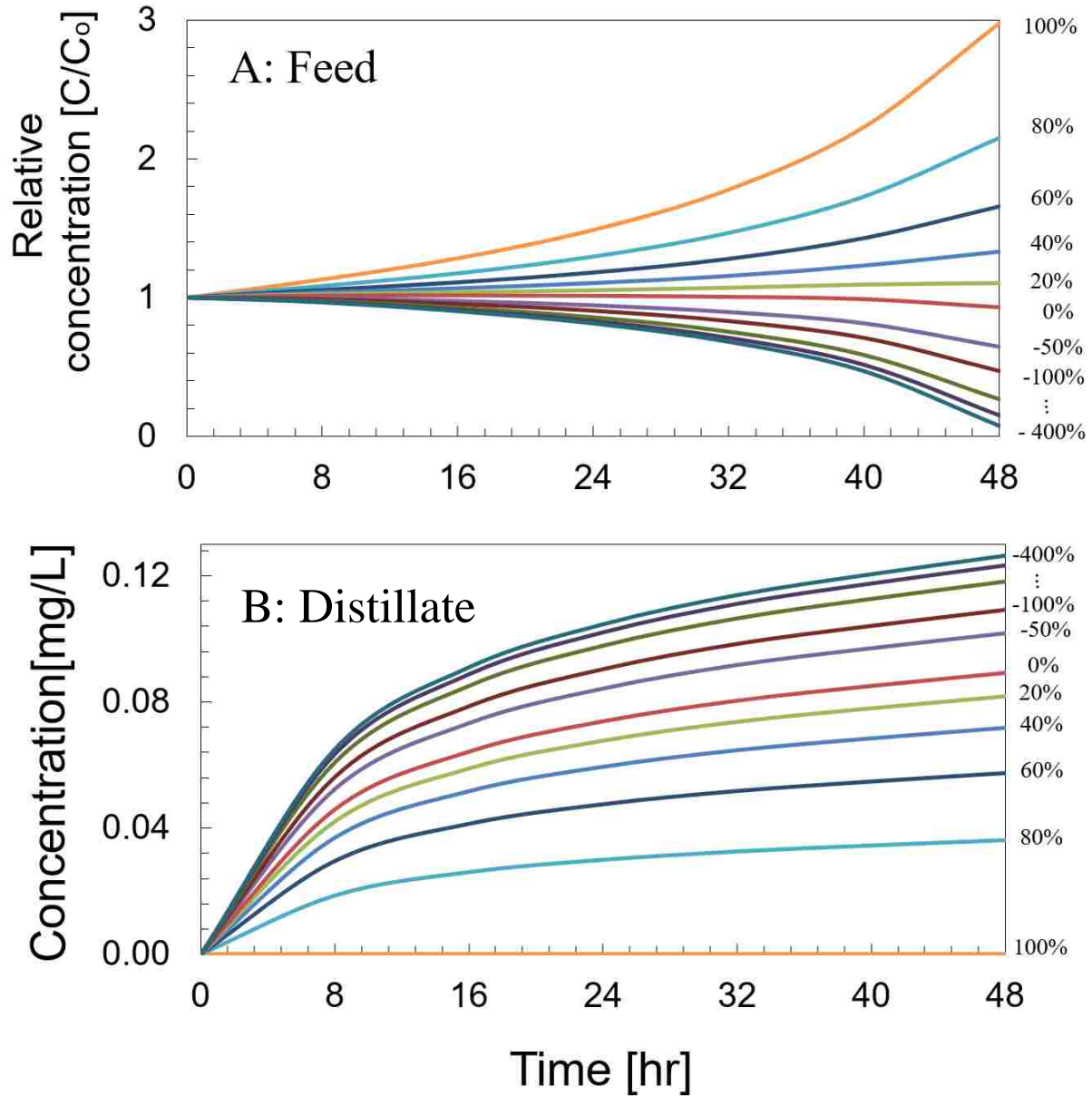
Figure 5. Theoretical rejection [%] models for the DCMD system, with rejection ranging from 100% to -400% in feed (A) and distillate (B), expressed as a function of time. Normalized concentrations (divided by initial concentration) are used for feed data, while observed concentrations [mg/L] are shown for the distillate.
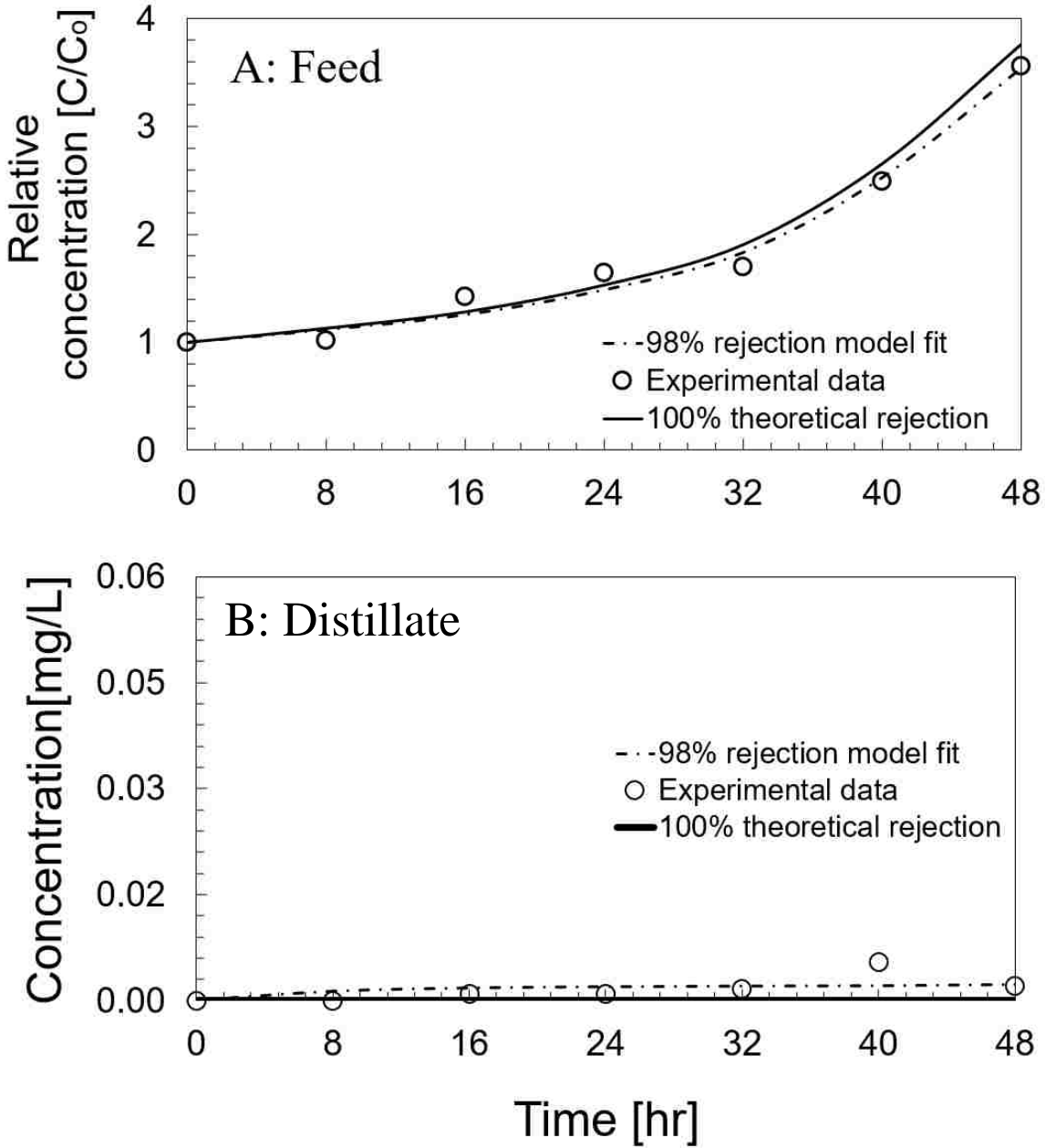
Figure 6. High rejection of 4-nitroaniline with concentration variation over time during DCMD. Black squares [O] represent observed concentrations for 48 hours, estimated concentration plots representing 100% theoretical rejection (solid line) estimated by mass balance both in (A) feed and (B) distillate are shown. Dashed line represents the rejection model fit determined by least square curve fitting method.
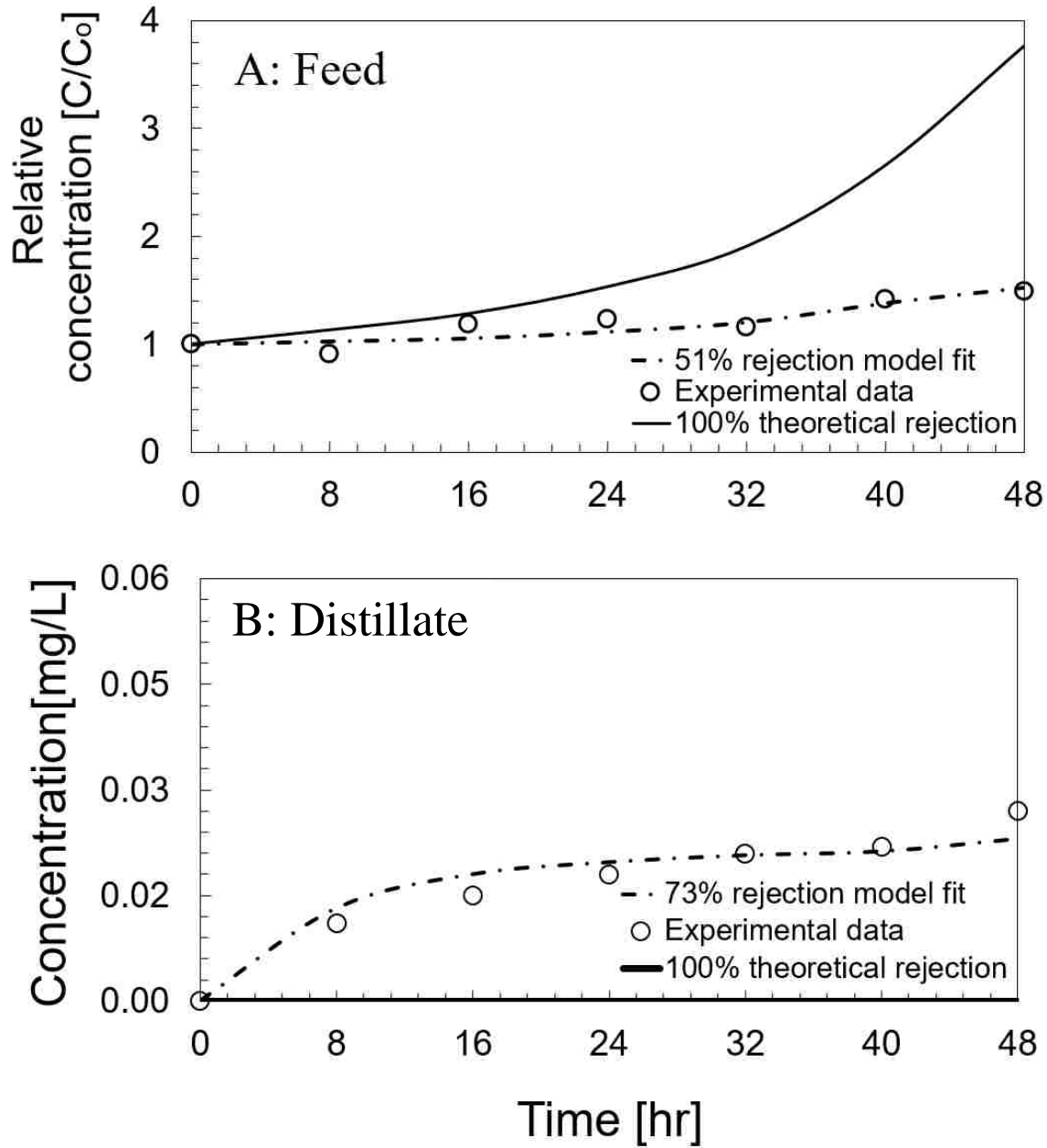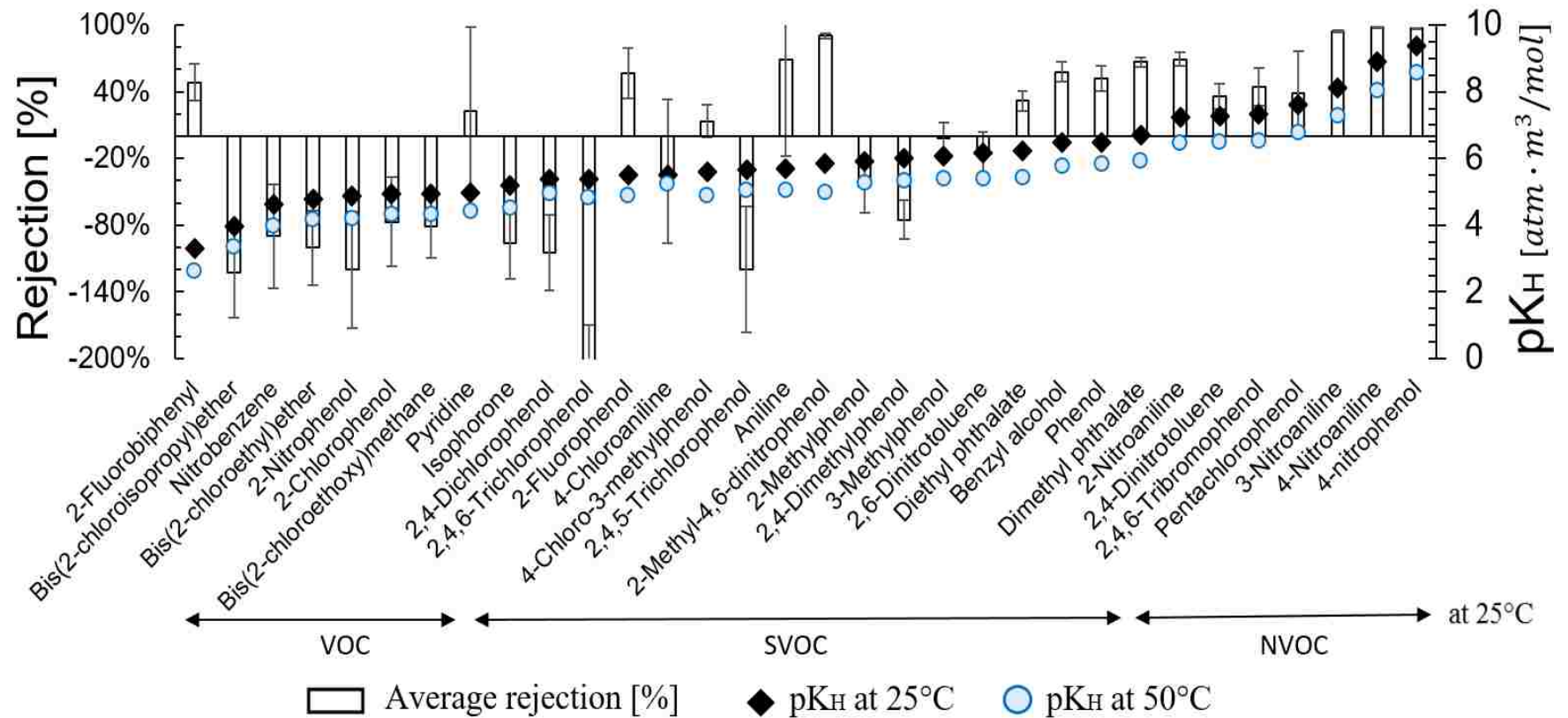
**Figure 7**. Intermediate rejection of benzyl alcohol with concentration variation over time during DCMD.
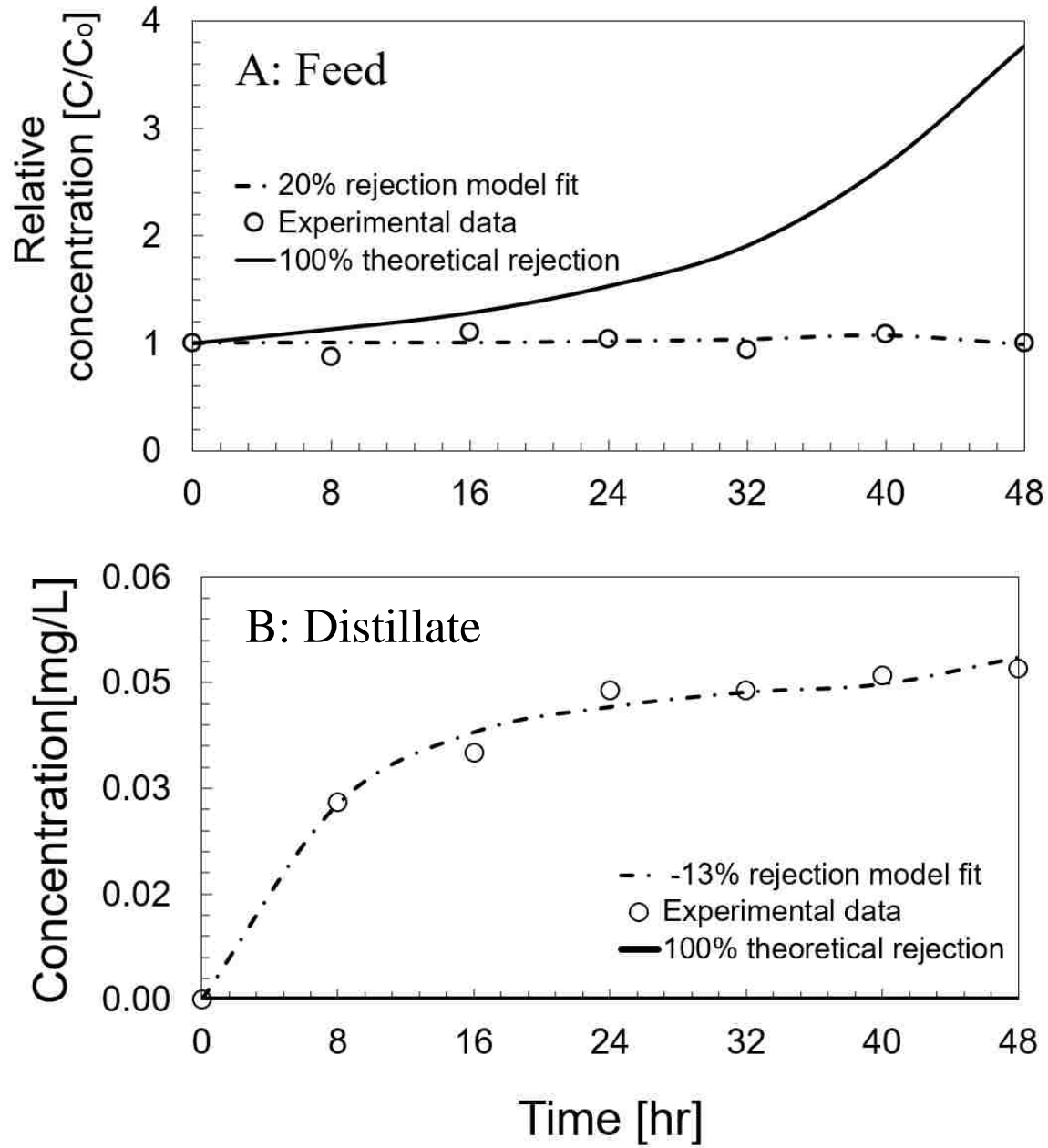
Figure 8. Modeled rejection of 3-methylphenol with concentration variation over time during DCMD.

Figure 9. Overall rejections of 32 semi-volatile and non-volatile organic compounds by DCMD plotted against their Henry's law constants values (shown as pK_H). Compounds with $5 < \text{p}K_H < 6.52$ and p$K_H > 6.52$ represent semi-volatile and non-volatile, respectively. Error bars represent standard deviations.
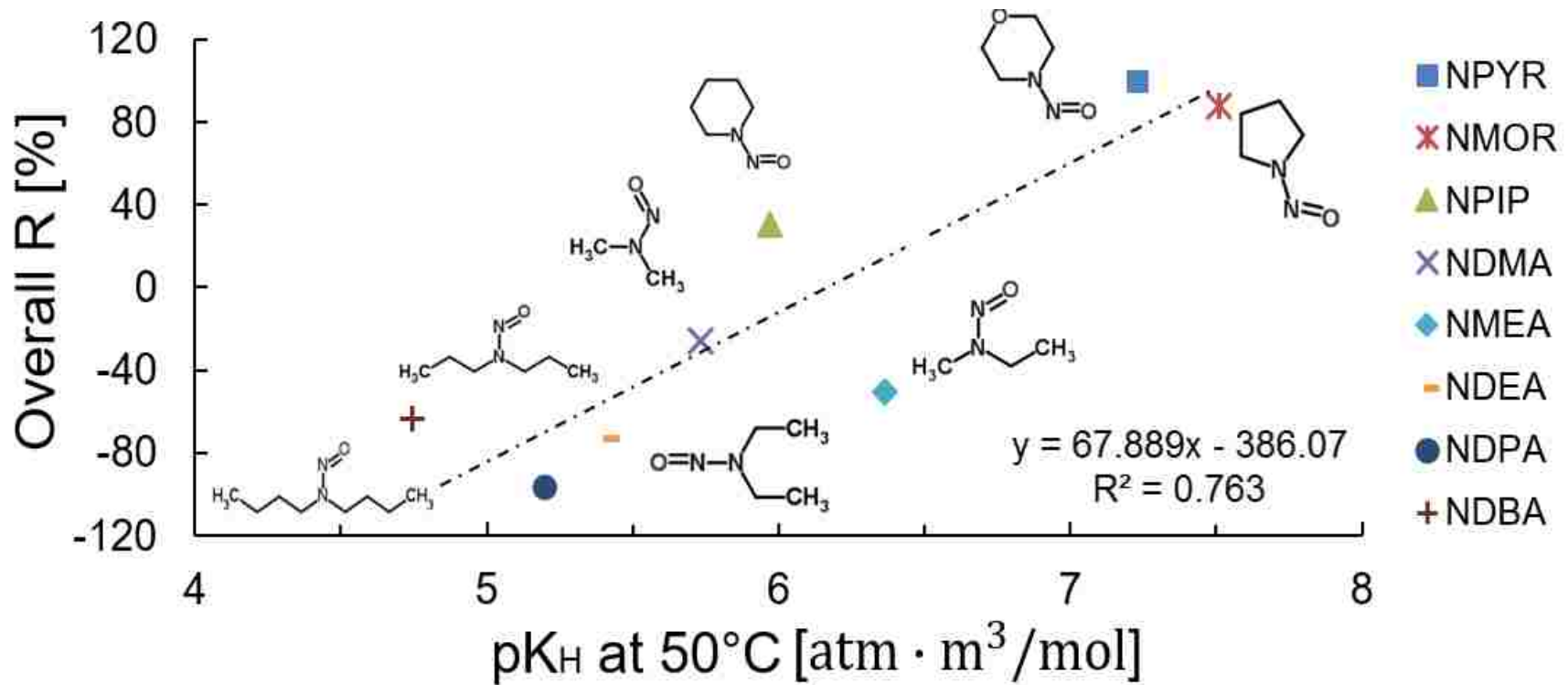
Figure 10. Overall rejections [%] of 8 nitrosamines with increasing Henry's law constants values shown as pK_H at 50°C. Abbreviations for compounds represent N-nitrosopyrrolidine (NPYR), N-nitrosomorpholine (NMOR), N-nitrosopiperidine (NPIP), N-nitrosodimethylamine (NDMA), N-nitrosomethylethylamine (NMEA), N-nitrosodiethylamine (NDEA), N-nitrosodipropylamine (NDPA), and N-nitrosodibutylamine (NDBA).
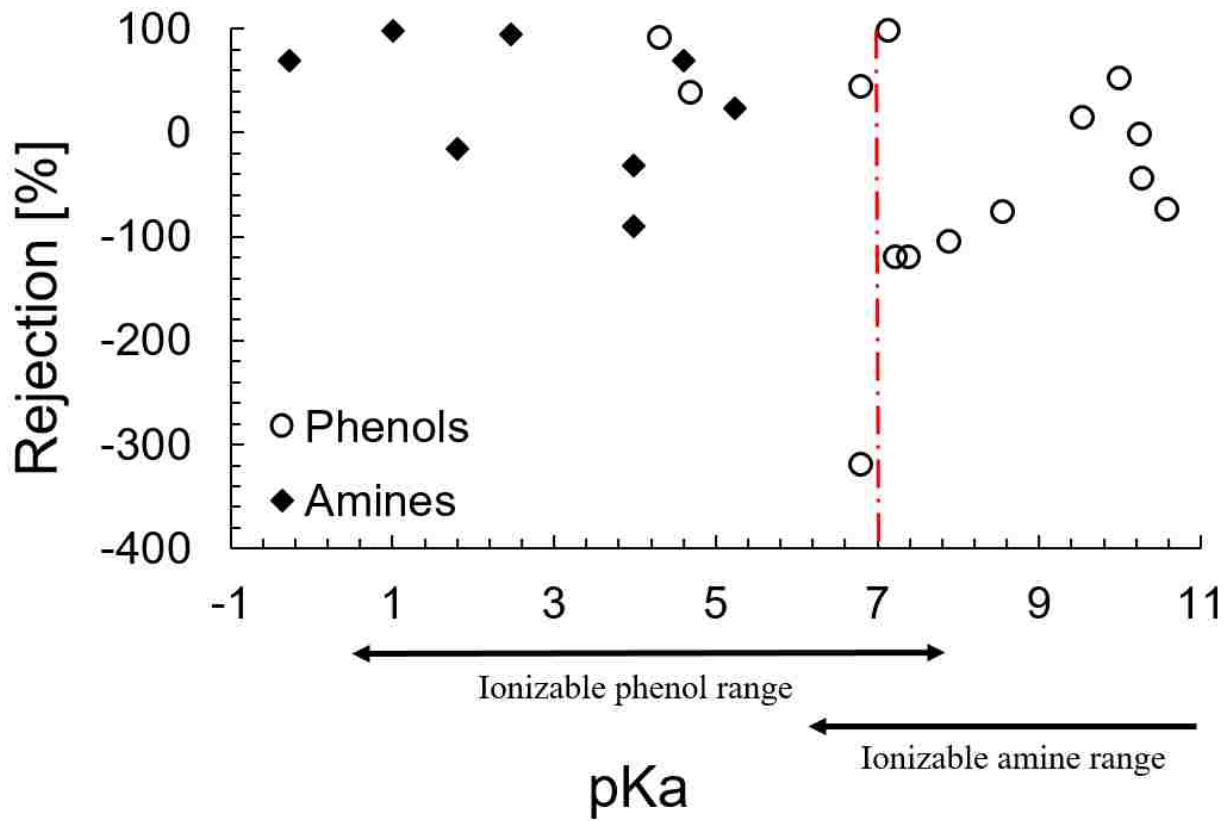
Figure 11. Rejections with dissociation effect (pK_a) for phenols and amines.
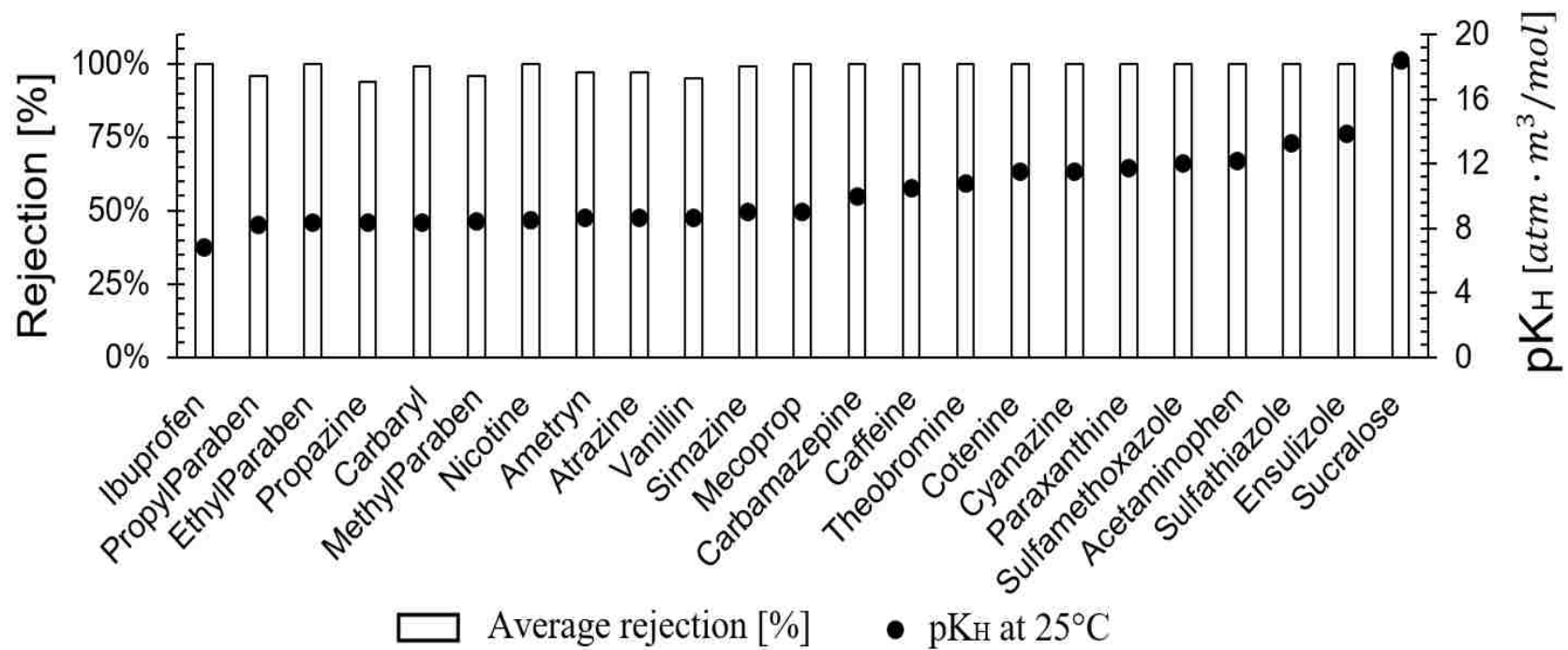
Figure 12. Overall rejection of 23 non-volatile PPCPs by DCMD, Henry's law constants values shown as pK_H at 25°C.
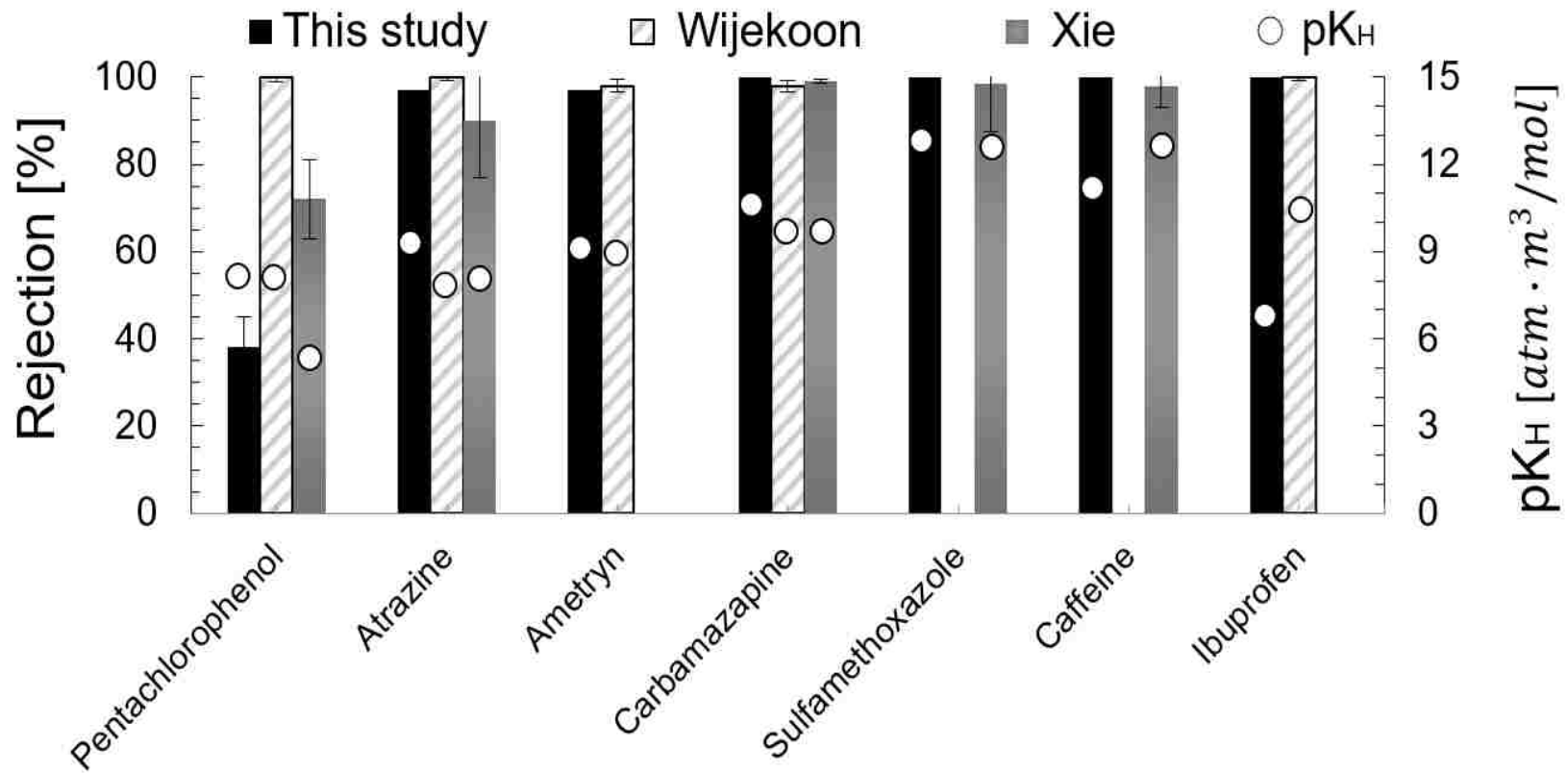
Figure 13. Comparison of rejection values and Henry's law constants (pK$_H$) between this study, Wijekoon[10], and Xie[11]. Experimental conditions in the paper, Wijekoon, and Xie during MD are at pH 7, pH 9, and pH 7.1, respectively. White circles represent Henry's law constants (pK_H). Error bars represent standard deviations. Sulfamethoxazole and caffeine were not evaluated by Wijekoon et al. Similarly, ametryn and ibuprofen were not evaluated by Xie et al.
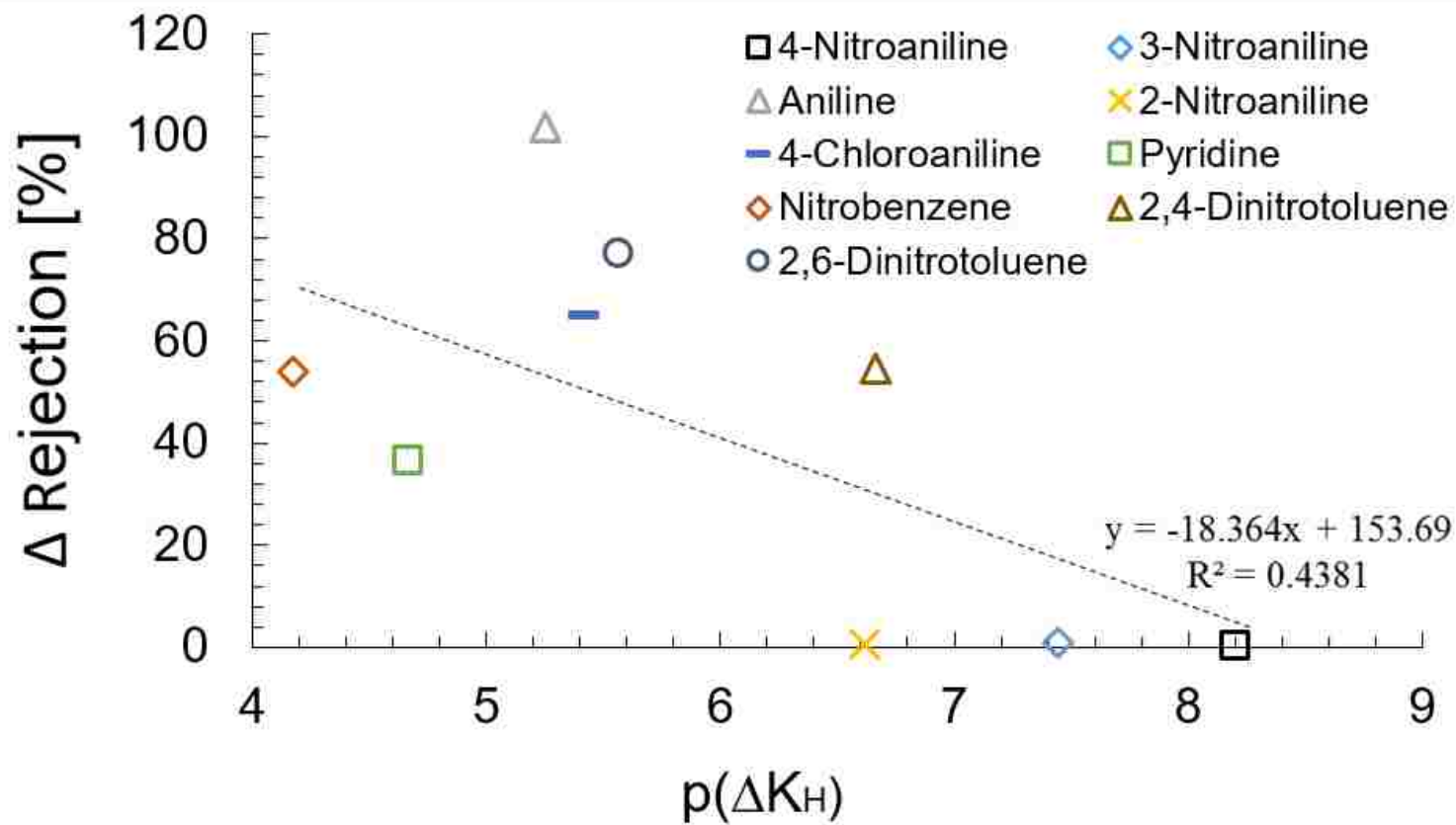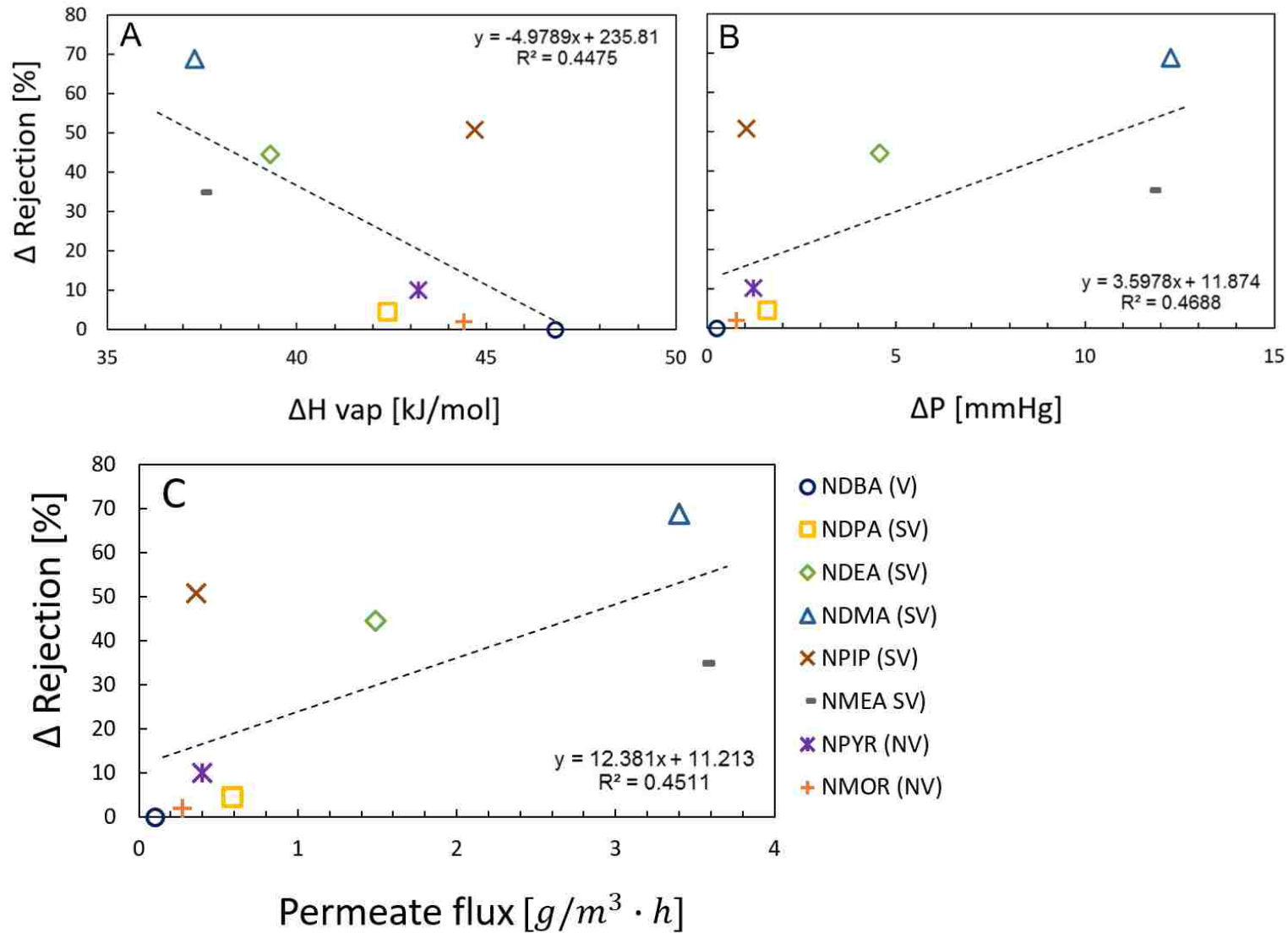
Figure 14. Correlation of Δ rejection in feed and distillate [%] versus $p(\Delta K_H)$ for an amine group.

Figure 15. Rejection differences for 8 nitrosamines between feed and distillate influenced by vaporization enthalpy (**A**), vapor pressure difference at 25°C and 50°C (**B**), and permeate flux (**C**)
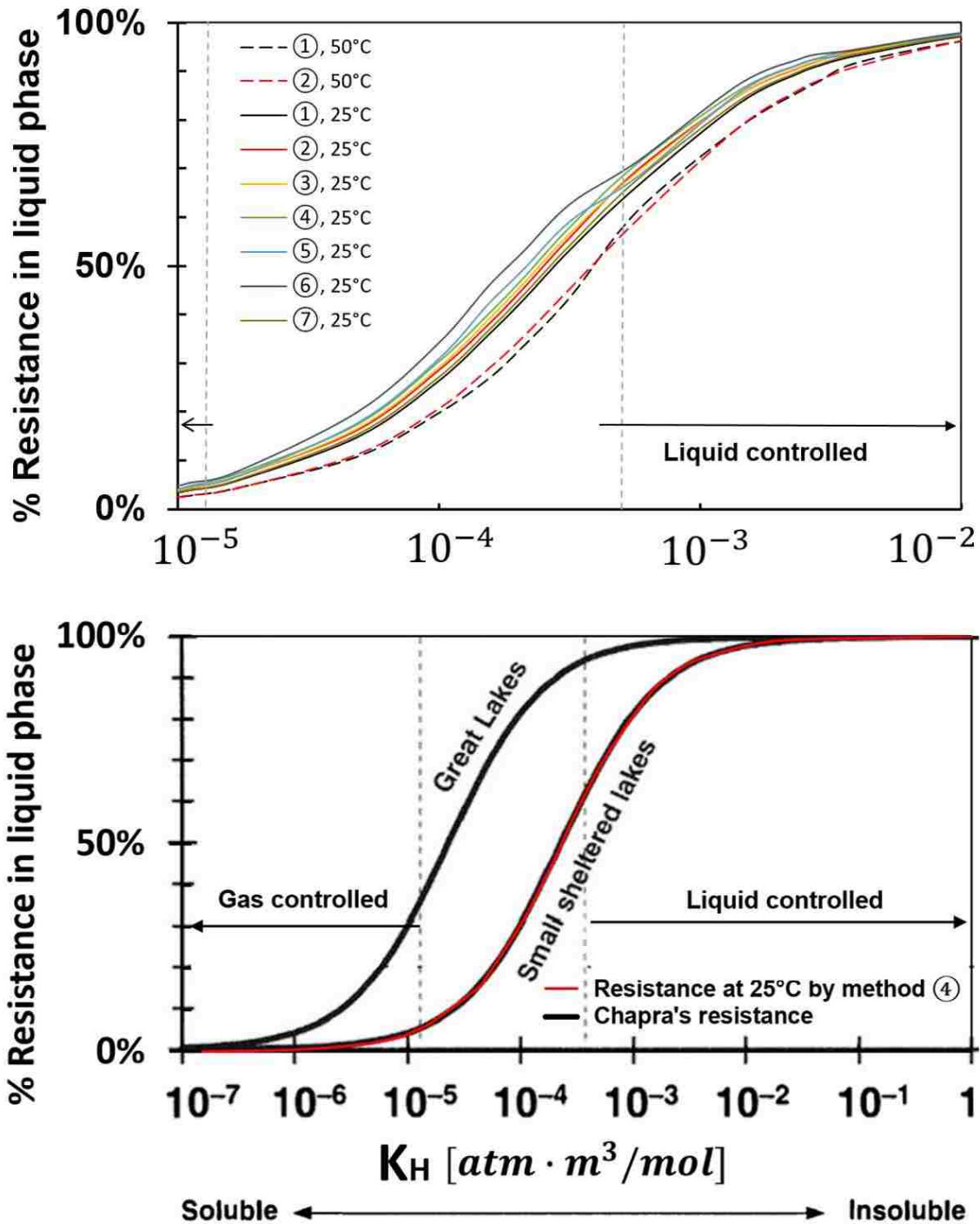
Figure 16. *Percentage resistance in liquid phase of volatiles and semi-volatiles organic compounds correlated with Henry's law constants (*K_H*). The percentage resistance* is quantified by using equation (7) with 9 approaches to calculate diffusivities at two temperatures. Chapra's resistance compared with the resistance calculated by fourth approach.